Australian Government
Geoscience Australia

Seismicity in the Southwest of Western Australia

Cvetan Sinadinovski

Record
2004/15

Geoscience Australia Record 2004/15

SEISMICITY IN THE SOUTHWEST OF WESTERN AUSTRALIA

by

Cvetan Sinadinovski

Geohazards
Geoscience Australia
GPO Box 378
Canberra ACT 2601

DEPARTMENT OF INDUSTRY, TOURISM AND RESOURCES

Minister for Industry, Tourism & Resources: The Hon. Ian Macfarlane, MP
Parliamentary Secretary: The Hon. Warren Entsch, MP
Secretary: Mark Paterson

GEOSCIENCE AUSTRALIA

Chief Executive Officer: Neil Williams

ISSN: 1448-2177
ISBN: 1 920871 10 1

GeoCat No. 48966

Bibliographic reference: Sinadinovski, C., 2004. Seismicity in the southwest of Western Australia. *Geoscience Australia Record* 2004/15.

CITIES PROJECT PERTH

SEISMICITY IN THE SOUTHWEST OF WESTERN AUSTRALIA

OBJECTIVE

In the Cities Project Perth, Geoscience Australia (GA) is developing a multi-hazard risk assessment of the Perth metropolitan area. One of the main objectives of the Project is to develop an earthquake hazard and risk model for this area. The hazard model is developed using information about earthquakes, the geology and the local soil characteristics of the region. As part of this process, we will develop several earthquake scenarios with events originating at specific locations in the region.

To define an appropriate model of seismicity, the Cities Project initiated an expert debate to discuss and to formulate geological and seismological parameters for the Southwest Seismic Zone and the area around Perth. The debate was followed by a workshop in December 2002 in Canberra where the seismicity model of SW WA was ultimately defined. Further discussion was held following the workshop, culminating in an agreed seismicity model for the region.

PARTICIPANTS IN THE DEBATE

GA - John Schneider*, Cvetan Sinadinovski*, Trevor Jones*, Phil Cummins*, Mark Leonard, Clive Collins*, Dan Clark*, Alan Whitaker*, Trevor Dhu, David Robinson* and Andrew Jones;

Guria Consulting – Brian Gaull*;

University of Western Australia – Mike Dentith;

Curtin University – Simon Wilde;

Geological Survey of Western Australia – Richard Langford;

ESS – Gary Gibson*, Amy Brown;

Melbourne University – Mike Sandiford;

Australian National University – Stephen Cox*, Kurt Lambeck, and Brian Kennett.

* - attended the Canberra workshop in December 2002

TABLE OF CONTENTS

INTRODUCTION

The aim of the debate was to develop appropriate earthquake hazard models for the Southwest part of Western Australia using up-to-date information about earthquake occurrence, geology and tectonic characteristics of the region known as the Southwest Seismic Zone. Utilising knowledge of seismicity and tectonic settings, the seismic source zones were determined and their seismic parameters used to develop hazard models.

In order to produce the hazard maps, our models require understanding of the tectonic processes which generate earthquakes and characterisation of the following parameters and their associated errors:

- frequency of earthquake;
- distribution of earthquakes with depth;
- maximum credible magnitudes for particular geological structures, and
- delineation of active faults.

Our new models subsequently will be used to calculate spectral accelerations and to produce maps for specific return periods.

DEFINITION OF TERMS

The purpose of a seismic hazard analysis is to assess the probability that the ground motion parameter at a site due to earthquakes from potential seismic sources will exceed a certain value in a given time period. The association of seismicity with the tectonic elements constitutes, where possible, a significant proportion of the earthquake hazard assessment. This and several other important issues have been given consideration during the assessment process:

- definition of the seismic zones and background seismicity in respect to the location of the seismic events;

- temporal variability of the seismic parameters;

- earthquake mechanisms and fault definition;

- potential for stress accumulation and release;

- geophysical measurements, etc.

GEOLOGY AND GEOPHYSICS

First we address the characteristics of the Southwest Seismic Zone in the context of Western Australian geology. The exact boundaries of the Southwest Seismic Zone are not precisely defined, but it lies within the Yilgarn Craton which is part of the Archaean Shield structure (Fig. 1). The southwest Yilgarn Craton, was previously subdivided by Gee *et al.*(1981) into the Western Gneiss Terrane (WGT), and two granite greenstone Provinces to the east, the Murchison and Southern Cross Provinces. Boundaries between the provinces were only approximately located but inferred to separate crust with contrasting geological attributes: particularly the relative abundance of older gneissic belts in the WGT, and the structural orientation and lithological content of greenstone belts in the Murchison and Southern Cross Provinces.

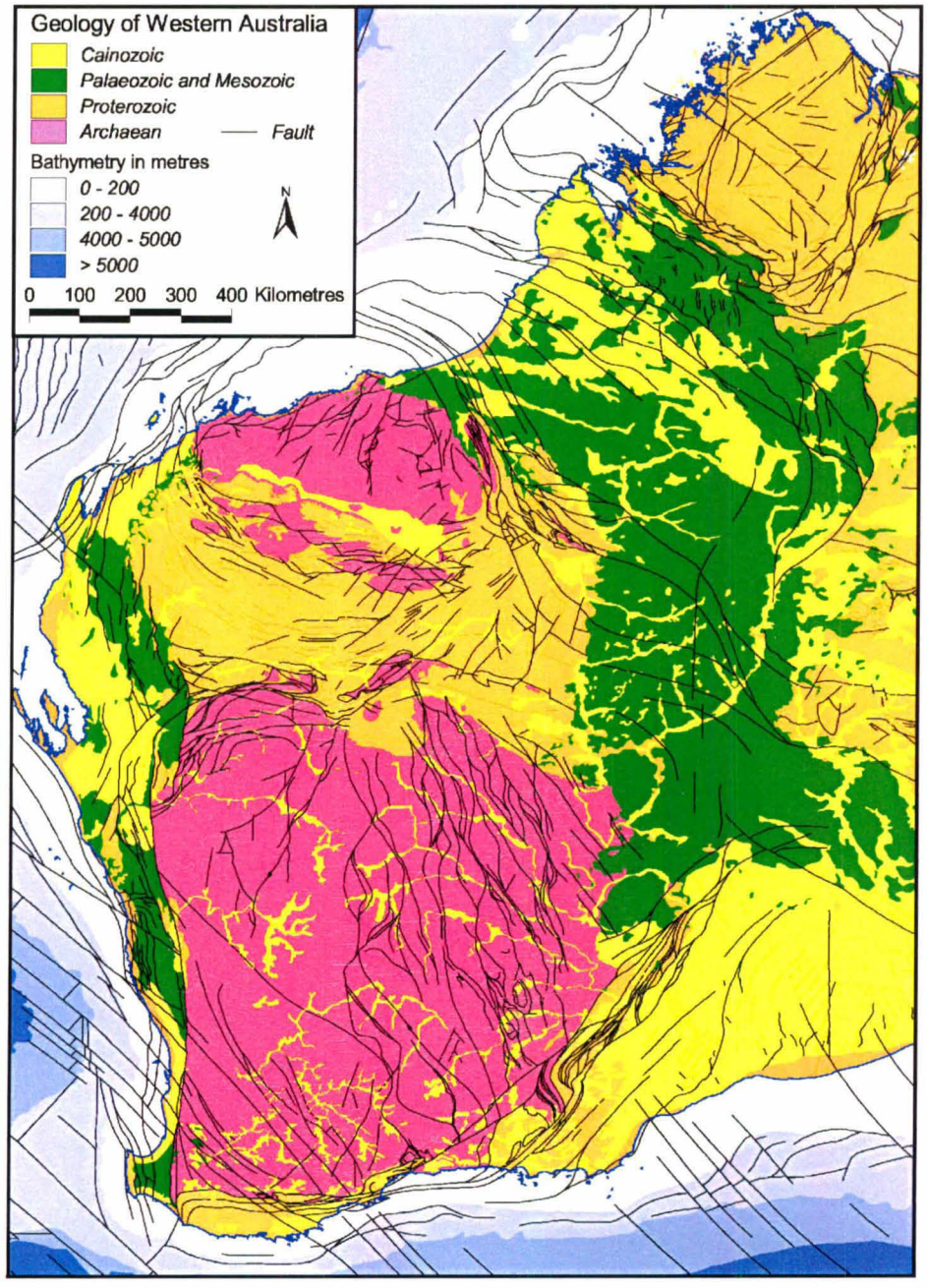

Figure 1: Geology of Western Australia

The absence of outcrop suggests the use of regional geophysical datasets for mapping large scale units and structures in the area (Fig. 2). These data have also been supplemented by higher resolution surveys undertaken for mineral exploration.

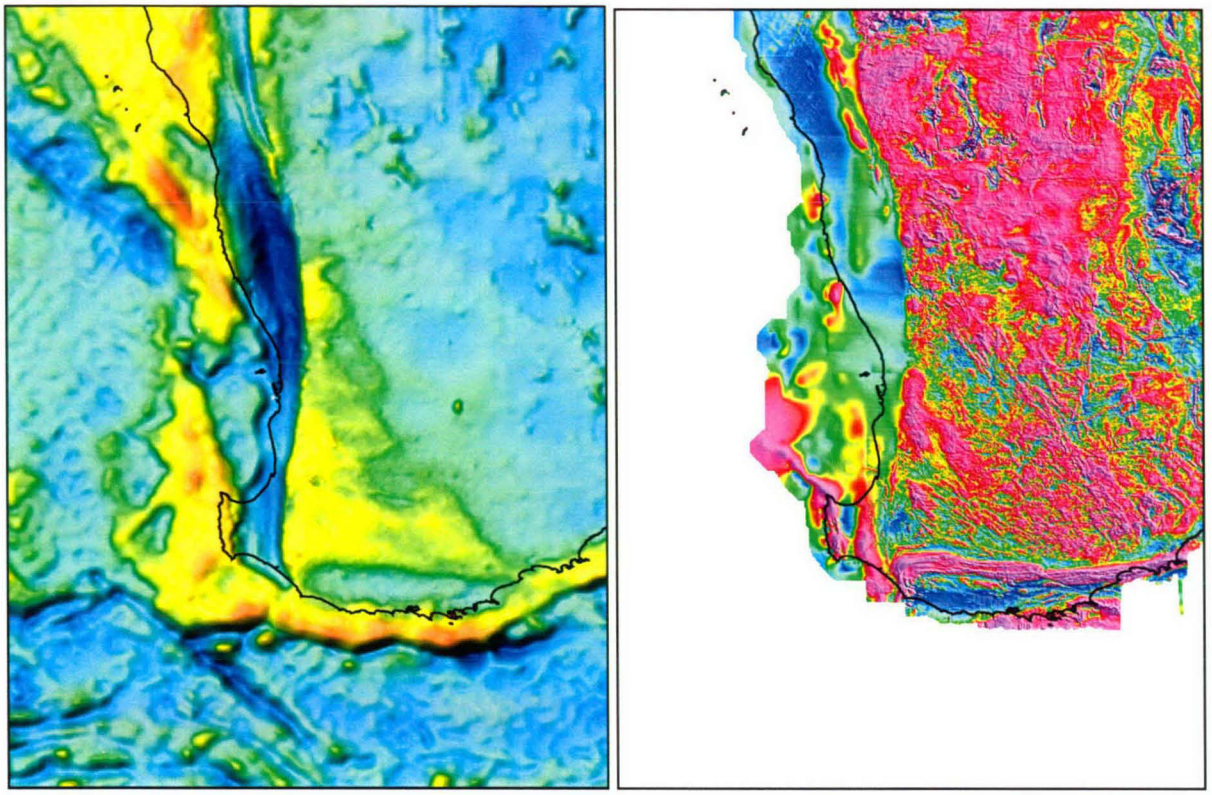

a b

Figure 2: Gravity (a) and Magnetic (b) anomaly maps of SW Western Australia

The region has been subdivided a little differently on the basis of more recent aeromagnetic interpretation (Whitaker, 1992; Whitaker and Bastrakova, 2002). In this model the Murchison domain in the north extends westward to the Darling Fault, the western boundary of the Yilgarn Craton, and is separated from the South West domain to the south by the north-northwest-trending Toodyay-Lake Grace domain. The Southern Cross domain bounds the Murchison and Toodyay-Lake Grace domains to the east.

The southern Murchison domain is characterised by extensive undivided gneiss-migmatite-granite (all of granitic composition) with little compositional banding. Rare greenstone and gneiss belts are oriented in a northerly direction. The southern part of the domain has been intruded by a suite of moderately- to highly-magnetised granite plutons that form a corridor approximately 100 km wide which is oriented west-northwest. Sparse regional faults transect the region with northerly orientations more common adjacent to the Darling Fault. However, it should be noted that resolution of structures is limited by the 1500m line-spacing of surveys in this area relative to that provided by higher quality surveys further east.

To the south the Toodyay-Lake Grace domain is characterised by abundant compositional banding attributed to gneiss. The compositional banding is grossly aligned with the local orientation of the belt which is largely northwest to north-northwest but includes a small

north-trending arm that bounds the Murchison domain in the southeast. Some large-scale tight to isoclinal folds are inferred and the domain is transected by several north-northwest-trending faults. The domain is located within a slightly broader zone of low pressure, granulite facies metamorphism. Boundaries of the Toodyay-Lake Grace domain with the Murchison domain to the north and South West domain to the south/southwest are complex.

The South West domain is triangular in shape being bound by the Toodyay-Lake Grace domain to the northeast, the north-trending Darling Fault in the west, and east-trending felsic and mafic granulites of the Albany-Fraser Province to the south. Much of the domain is composed of low to moderately magnetised undivided gneiss-migmatite-granite with little compositional banding evident. A small region adjacent to the Darling Fault in the southwest of the domain, with general low magnetisation but common compositional banding, corresponds with the Ballingup metamorphic belt. Sparse poorly magnetised greenstone remnants throughout the domain are small and are largely not resolved in the regional aeromagnetic data. The South West domain has been intruded by several moderately- to highly-magnetised granite plutons, particularly adjacent to the Darling Fault. Large-scale regional faults are evident throughout the domain. West-northwest fault orientations are most common in the southwest while northwest, northeast and east-northeast orientations are more common further to the east. Abundant east-trending fractures are evident adjacent to the southern boundary of the domain. The southern margin of the domain is also demagnetised for 20 to 50 km north of this boundary as a result of thrusting of the Albany–Fraser Province during the Proterozoic (Whitaker, 1992).

The Southern Cross domain is located to the east of the Murchison and Toodyay-Lake Grace domains. The domain is largely composed of poorly magnetised, undivided gneiss-migmatite-granite but includes abundant very poorly magnetised greenstone belts. The greenstones include some highly magnetised units of banded iron formation and ultramafic rocks. The greenstones have been deformed so that they describe sinuous north-northwest to north-northeast trending belts. Poorly to highly magnetised granite plutons are relatively abundant, particularly in the south of the domain. North-northeast and east-west trending regional faults are abundant in the domain. Demagnetisation of the southern margin of the domain is more extensive (to 90 km from the boundary) adjacent to the Albany Fraser Province than for the South West domain.

The gravity data of southwestern Australia consist of the national 11 km grid in-filled by government and industry surveys, to about 5 km average spacing, in a 200 km wide corridor abutting/paralleling the western coast line. These data provide complementary but significantly lower resolution information than the regional aeromagnetic coverage. The combined gravity and magnetics anomaly images are given in Fig. 3 and 4.

The average Bouguer gravity anomaly associated with much of the Murchison and Southern Cross domains is in the order of –450 um/sec^2. Local gravity highs to –100 um/sec^2 in this region correlate with greenstone belts. A major north-northwest trending gravity gradient (the Yandanooka-Cape Riche Lineament of Everingham, 1968) with high values to the south west transects the South West domain and the north west of the Toodyay-Lake Grace domain. The high gravity to the south west of the gradient has been linked with crust of higher average thickness and a thick, high seismic velocity, high density basal layer relative to crust to the east (Mathur, 1976). Certainly there is no inferred change in surface geology across the position of this lineament as inferred from interpretation of aeromagnetic data. However,

Wilde *et al.* (1996) have interpreted/mapped a zone with abundant migmatite immediately east of the gravity lineament.

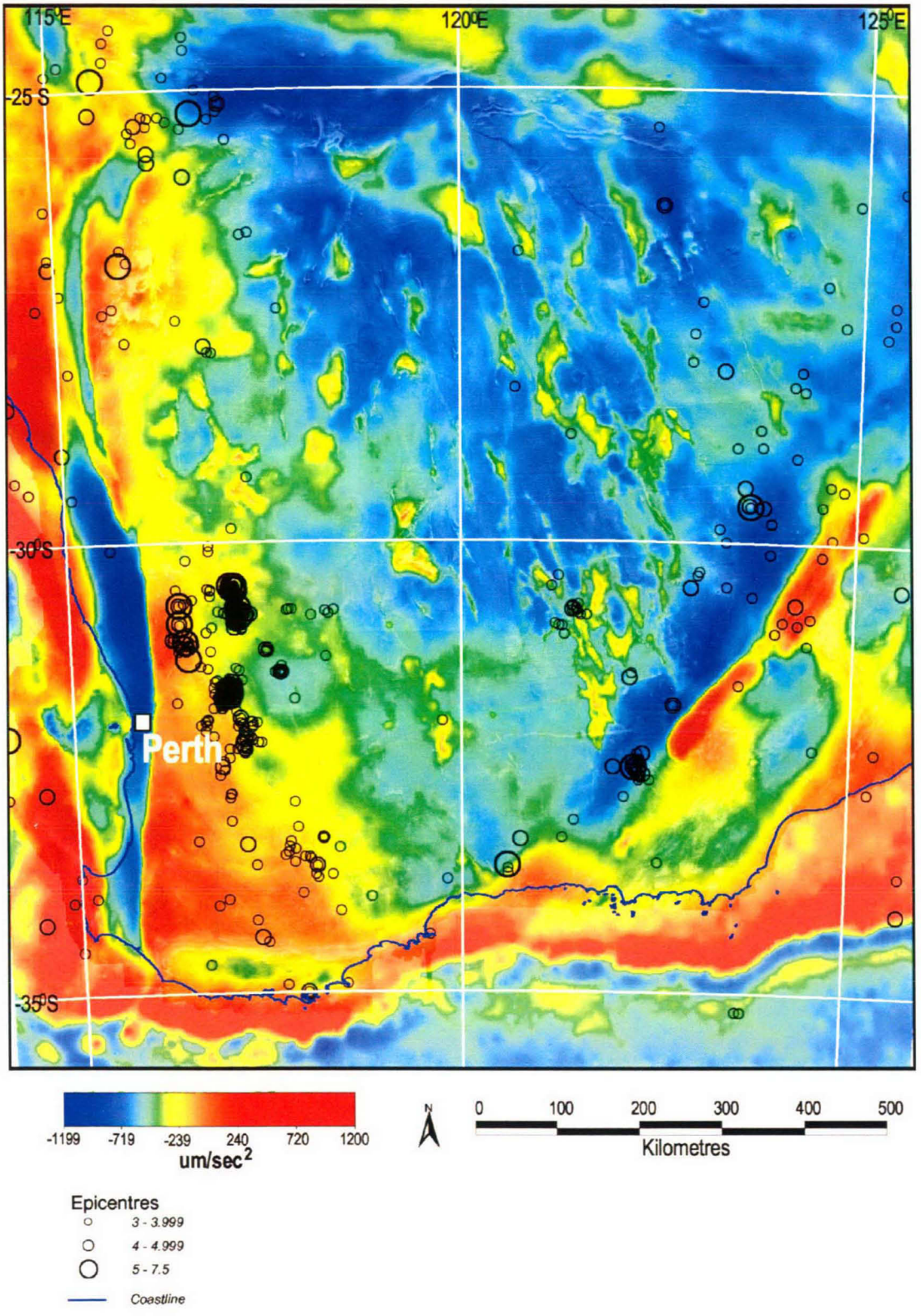

Figure 3: Combined gravity/magnetics image with seismicity for Southwest WA (courtesy of de Beers Australia Ltd)

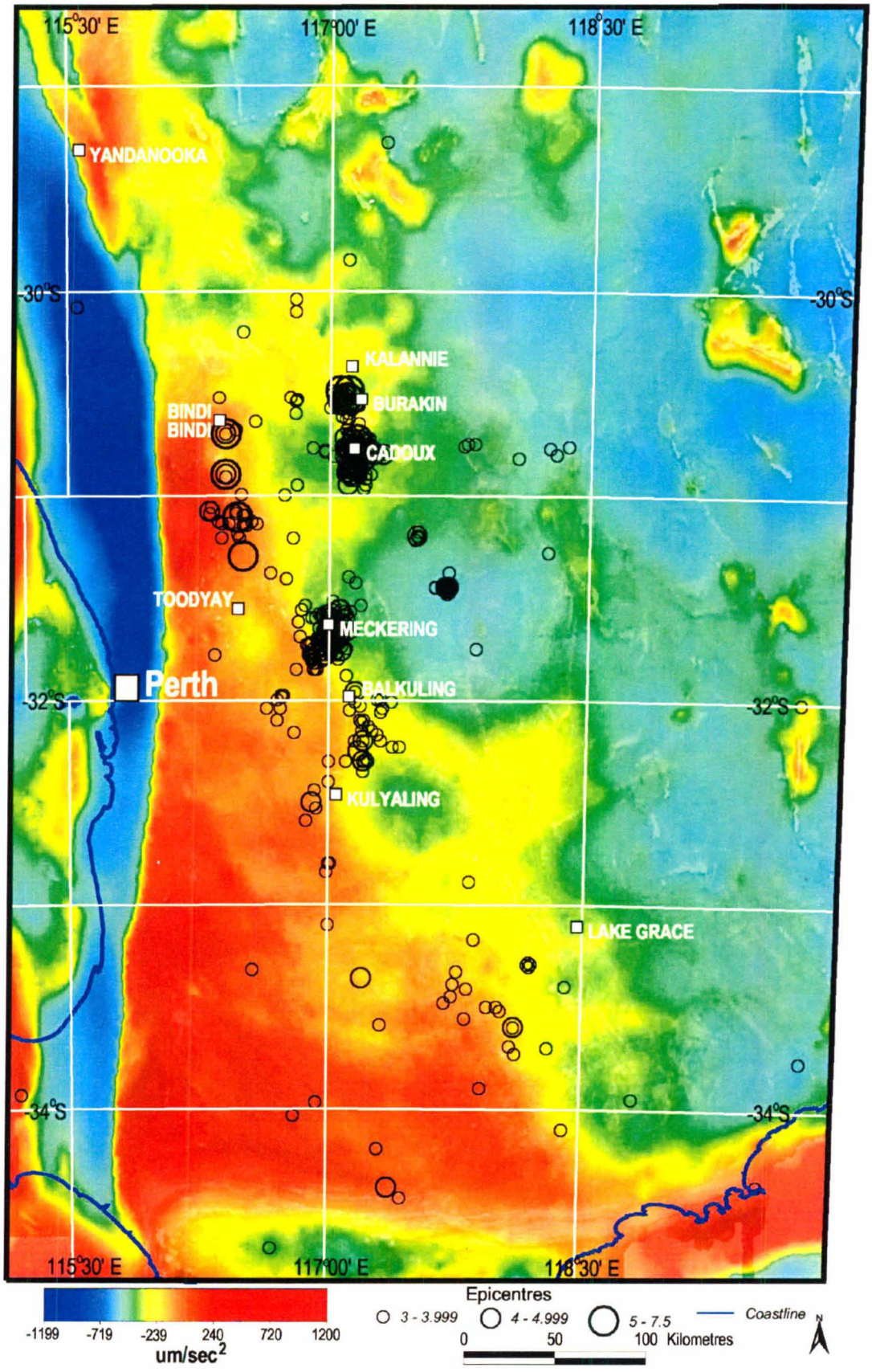

Figure 4: Combined gravity/magnetics image with seismicity around Perth (courtesy of de Beers Australia Ltd)

The highest incidences of earthquake epicentres in the region are centred on Meckering, within the Toodyay-Lake Grace domain, and Cadoux in the southern Murchison domain as shown in more details in Fig. 4. A zone of relatively high epicentre incidence, which includes these two areas of highest incidence, describes an 's' shaped form (Cadoux-Kondut-Yerecoin-Bolgardt-Mekering-Balkuling-Kulyaling) from 180 km northeast to 110 km southeast of Perth. The epicentres from Meckering to Kulyaling correlate strongly with structural trends of the Toodyay-Lake Grace domain as inferred from interpretation of aeromagnetic data. This area also correlates very well a local curve and more general north-northwest trend of the major gravity gradient (Yandanooka-Cape Riche Lineament) through the area. Further south, earthquake epicentre incidence is relatively abundant across the South West domain but particularly so between the Yandanooka-Cape Riche Lineament and the southwestern boundary of the Toodyay-Lake Grace domain.

More generally, the incidence of epicentres in the southern Murchison and South West/Toodyay-Lake Grace domains drops off extensively east of the western boundary of the Southern Cross domain. Epicentre abundance also drops significantly north of an east-northeast-trending gravity lineament that passes through the central Murchison domain near the towns of Bindi Bindi, Damboring, and Kalannie. Figure 5 represents the Southwest of WA in more detail where epicentres are superimposed on the fault structures as defined by the geological map of the Geological Survey of Western Australia (Myers and Hocking, 1998).

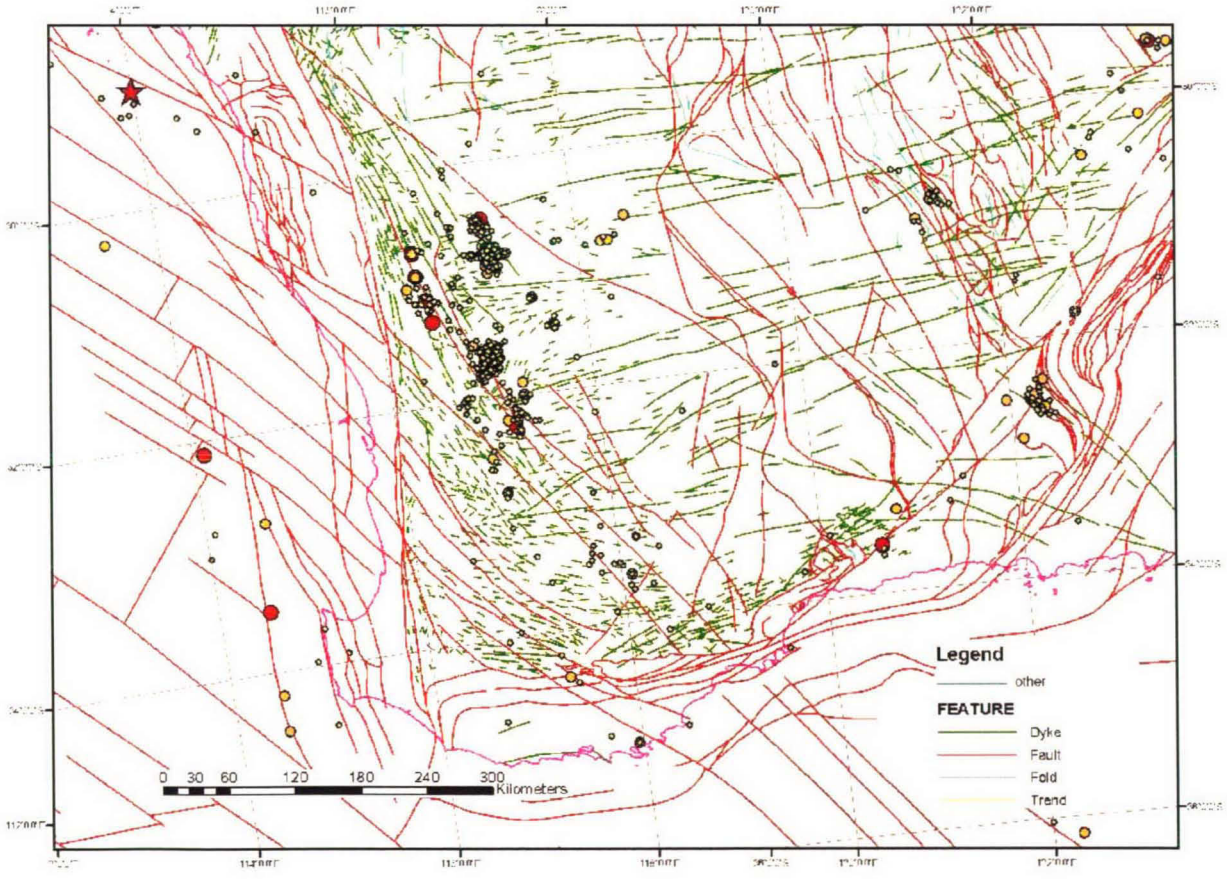

Figure 5: Seismicity and faults in the SW Western Australia

REGIONAL SEISMOLOGY

The seismological data comprised subsets of Geoscience Australia's QUAKE Earthquake Database for Australia for the region around Perth (Fig. 6), the isoseismal maps (Appendix A) for the larger events and their fault plane solutions (Appendix B).

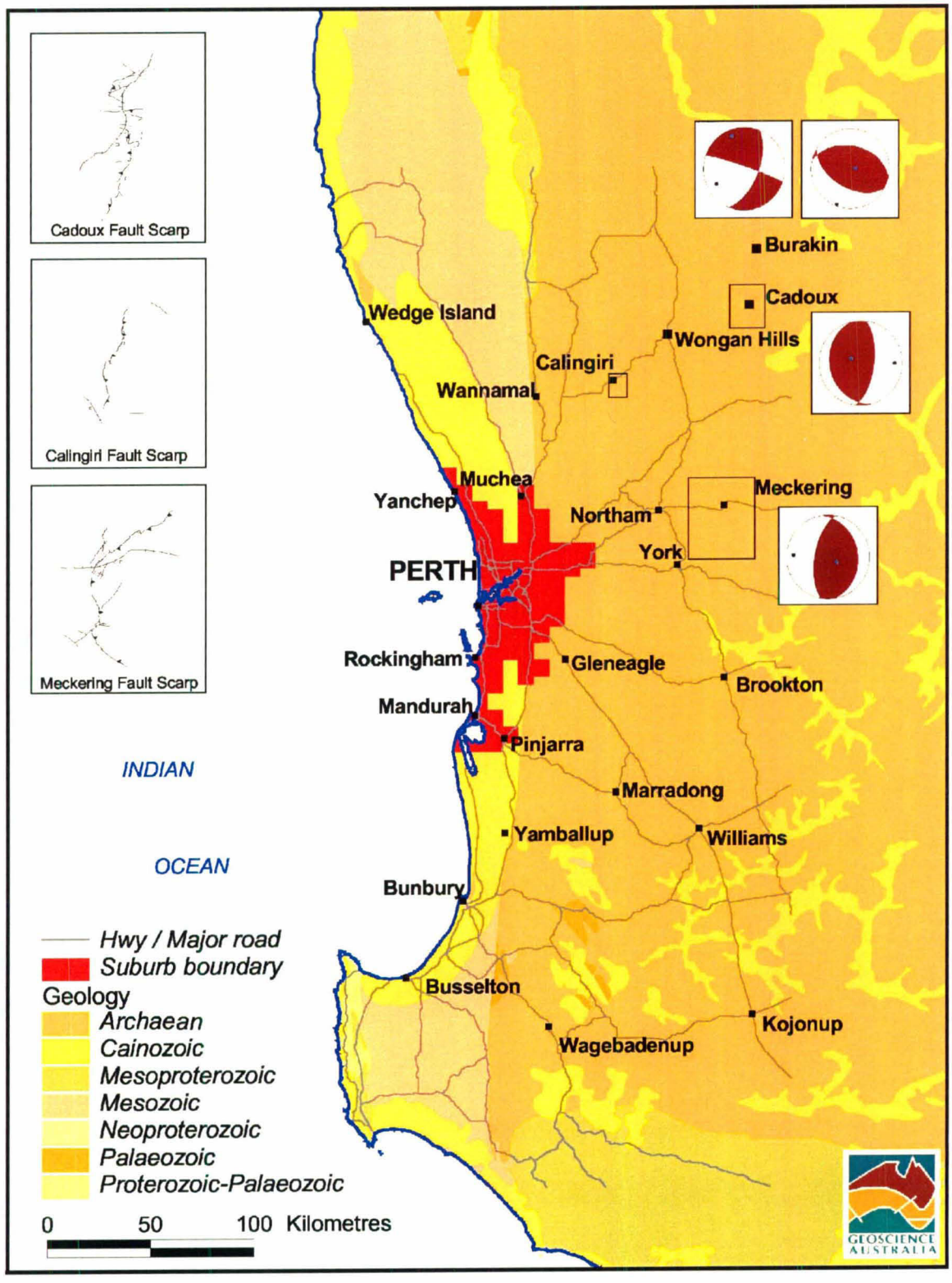

Figure 6: Geology of the wider Perth region with indication of the three largest earthquakes; fault plane solutions are shown for Meckering, Cadoux and Burakin

Seismicity parameters have been estimated only for those times in which the seismic network has been able to consistently record all earthquakes above the specified magnitude threshold on the Australian continent. In the preliminary analysis for this study the numbers of earthquakes were counted for the declustered dataset of various magnitude ranges in intervals of 0.2 which is about the uncertainty in magnitude. The dataset referred to as a declustered data set has the same magnitude ranges but the identifiable foreshocks or aftershocks are removed. A quake was considered to be a foreshock or an aftershock and was removed if it was within a certain distance of the main shock in a procedure described by Sinadinovski (2000).

Three large earthquakes have caused considerable destruction and surface ruptures in the Southwest Seismic Zone. They are the Meckering 1968 earthquake magnitude 6.9, the Calingiri event of 1970 magnitude 5.9 and the Cadoux earthquake of 1979 magnitude 6.2.

The original formation of the earthquake source zones was based on the work of Gaull *et al.* in 1990 as described in Appendix C. The epicentral data in the current GA catalogue appear to fit the source zones chosen by Gaull *et al.* (1990) reasonably well, even though an estimated 50% of the events have occurred since they were originally defined. Some modifications were done to the original source zone boundaries, namely the northern border of the Cadoux-Meckering zone, to include the most recent activity in the Burakin area.

The possible causes of intra-plate seismicity in the southwest of Western Australia are discussed separately (Appendix D), and although several mechanisms are proposed, none could be described as causal without considerably more information and analysis being made available.

Two models for seismic zoning were proposed in the workshop in December 2002:

- Model-I (Fig. 7), comprising

  a) Cadoux-Meckering zone, or Zone 1, modified from Gaull *et al.* (1990) to include the latest Burakin events;
  b) Larger zone east of Darling Fault, or Zone 2, with modified borders from Gaull *et al.* (1990) to follow closely the Darling Fault and the orientation of the main geological structures;
  c) Yilgarn zone covering the remainder of the Yilgarn craton;
  d) Offshore zone, or Zone 3, as part of the continental margin, modified from Gaull *et al.* (1990); and
  e) Perth basin, or background zone, as part of the continental shelf, modified from the EPRI 1994 report and Gibson and Brown's model called AUS5 discussed at the Australian Earthquake Engineering Society conference in 2002.

Note: Model-I had two versions: the first version when seismic parameters were calculated separately for Zone 2 and the Yilgarn zone, and second version when Zone 2 and the Yilgarn zone were combined as one zone.

- Model-II to be a smoothed version of Williams and Leonard's approach (Fig. C3), when seismic parameters for the Southwest zone are re-calculated for finer grid [1^{o}x1^{o} cells] where possible.

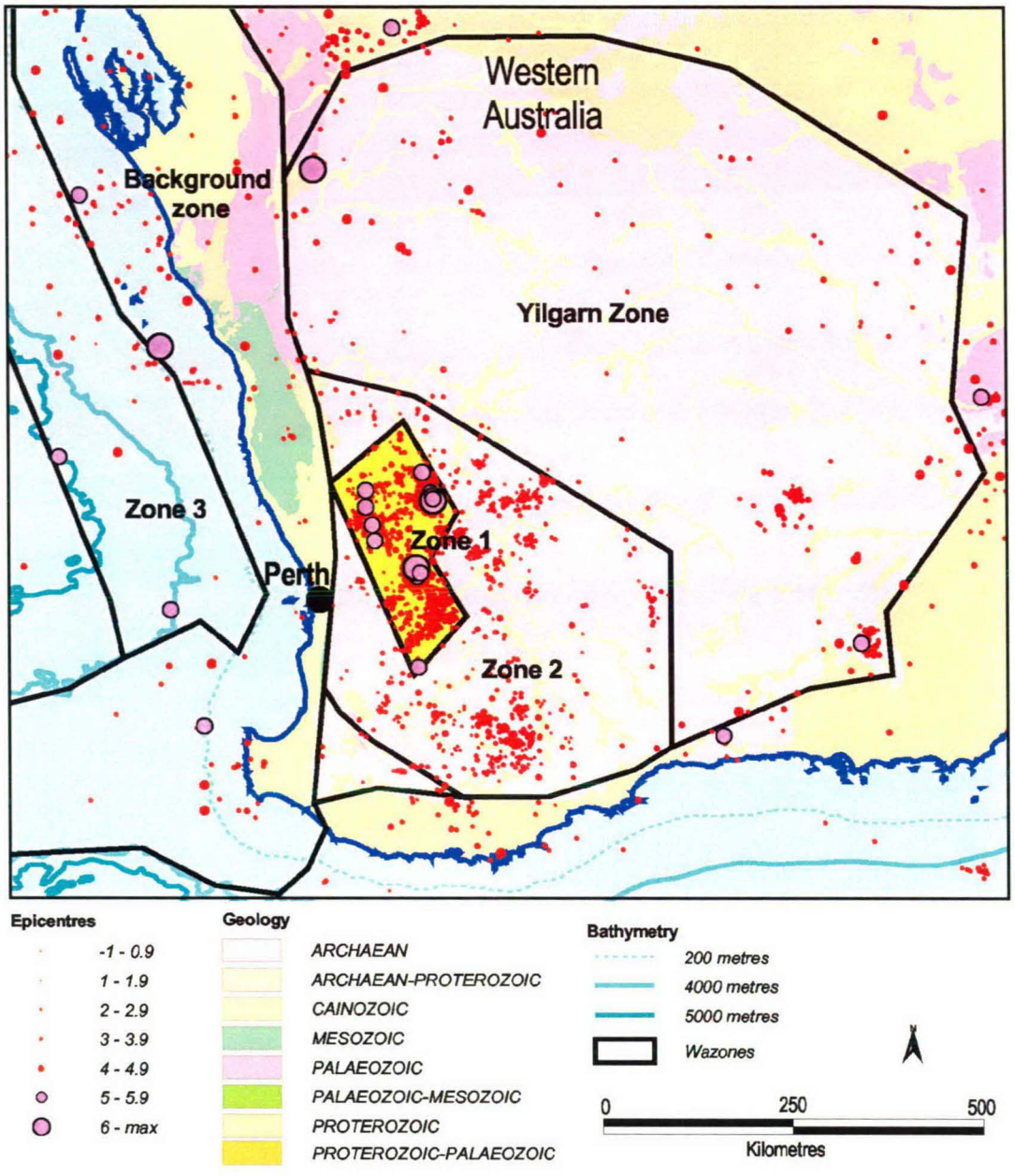

Figure 7: Seismic source zones of Southwest WA

The other recommendations for the seismic parameters to be used in the hazard calculation program are summarised below:

Maximum magnitude: Two options were anticipated

- Option-I where maximum moment magnitude of M_W 7.5 was assigned to all of the zones, including the background;
- Option-II where maximum moment magnitude of M_W 7.0 was assigned to Zones 1 and 2, and M_W 8.0 to Zone 3 and the background (Perth) zone.

Event depth: Two distributions of earthquakes were anticipated

- Distribution-I depths between 0 and 20 km for areas east of the Darling Fault;
- Distribution-II depths between 0 and 15 km for areas west of the Darling Fault.

The probabilistic distribution for the depth dependencies were not defined more specifically by the group of experts. GA is considering using a distribution with maxima in the top 5 km and decreasing with depth.

Fault type: Two types of faults were anticipated

- Reverse faults - 80% of the earthquakes will occur on reverse faults aligned with the structural trend NNW-SSE; and
- Strike slip – 20% of the earthquakes will occur on strike slip faults.

Variation of +/- 30° around these principal fault orientations was allowed..

Fault dip: Two positions of fault dips were anticipated

- Position-I - 50% of the earthquakes occur on faults dipping 35° East; and
- Position-II - 50% of the earthquakes occur on faults dipping 35° West.

Deterministic scenarios: For validation of hazard results only these two scenarios were selected to be simulated

- Meckering earthquake with moment magnitude M_W 7.0;
- Offshore event, 100 km west of Freemantle with moment magnitude M_W 6 (similar to the 1980 earthquake).

RECURRENCE RELATIONSHIP

The relation between the number of earthquakes and their magnitude is routinely approximated by the Gutenberg and Richter empirical formula (1949) represented by a single straight line in log-linear coordinates

$$\log N = a - bM \qquad ...(1)$$

where N is usually the cumulative number of earthquakes per year, M is the local or Richter magnitude and a, b are constants related to the total number of earthquakes above certain size and the frequency relation between small and large earthquakes. Data are treated by grouping of N according to the magnitude range.

Because earthquake size is characterised by seismic moment, one must know the relationship between the Richter and moment magnitude. This relationship may be developed empirically, but in the absence of quality data for large earthquakes in Australia we adopted curvilinear relationship (EPRI report, 1993) to convert from local magnitude M_{Lg} to moment magnitude M_W:

$$M_W = 3.45 - 0.473M_{Lg} + 0.145M_{Lg}^2 \qquad ...(2)$$

Although magnitudes measured in Australia are typically local magnitudes, M_L, rather than M_{Lg}, they are assumed to be equivalent for the purpose of this study, because just magnitude itself has an average uncertainty of ±0.5.

The coefficient b usually takes a value around 1. In general this relationship fits the data well on global scale, but not for particular tectonic regions. Various authors have discussed the spatial variation in b. In his work Kárník (1971) mentioned that in some cases for the weakest and the strongest earthquakes, the (log N, M) distribution deviated significantly from linearity. Recently, some other approximation formulae for that deviation have been applied (for example Utsu, 1999).

For use in prediction and comparative mechanism studies, standard errors of *b* must be supplied for statistical tests. Because earthquakes follow stochastic processes and the *b* value is a random variable, the probability distribution and the variance of *b* are essential in studying its temporal and spatial variation. The *b* value can be calculated by least-squares method (LSM), but the presence of even a few large earthquakes influences the resulting *b* value significantly. As an alternative, the maximum likelihood estimate (MLE) can be used to calculate *b* because it yields a more robust value when the number of infrequent large earthquakes is considered. Weichert (1980) discusses in detail the advantages and disadvantages of the various methods.

The data used for this study comprised a subset of GA's earthquake database for Australia. Analysis was restricted to only those time intervals in which the seismic network was able to consistently record all earthquakes of the specified magnitude. On our assessment, the periods of completeness were: 1901-present for $M \geq 6.0$, 1959-present for $M \geq 5.0$, 1965-present for $M \geq 4.0$, and 1980-present for $M \geq 3.2$ (Sinadinovski, 2000). Values of *a* and *b* coefficients for our preferred model with maximum magnitude M_W 7.5 in Western Australia using seismic data up to 1st of July 2002, are presented in Table 1.

Table 1: Seismic parameter values for zones closest to Perth

Source zone	Area (km^2)	M_{min}	M_{max}	b	A_{min}
Zone 1	25,365	3.9	7.5	1.00	3.266
Zone 2	134,344	3.9	7.5	1.00	0.252
Zone 3	330,916	3.9	7.5	1.00	3.617
Background	373,291	3.9	7.5	1.00	1.649
Yilgarn	460,465	3.9	7.5	1.00	1.970

M_{min} is the minimum moment magnitude, M_{max} is the upper bound magnitude, and A_{min} is the number of earthquakes per year with $M \geq M_{min}$ (intercept of equation (1) at $M=M_{min}$)

The level of seismicity normalised to 10,000 km^2 for the areal zones is shown in Fig. 8. This new configuration increases seismicity in the Zone 1 at the expense of decrease of seismicity in Zone 2, when compared with the earlier model of Gaull *et al.* 1990.

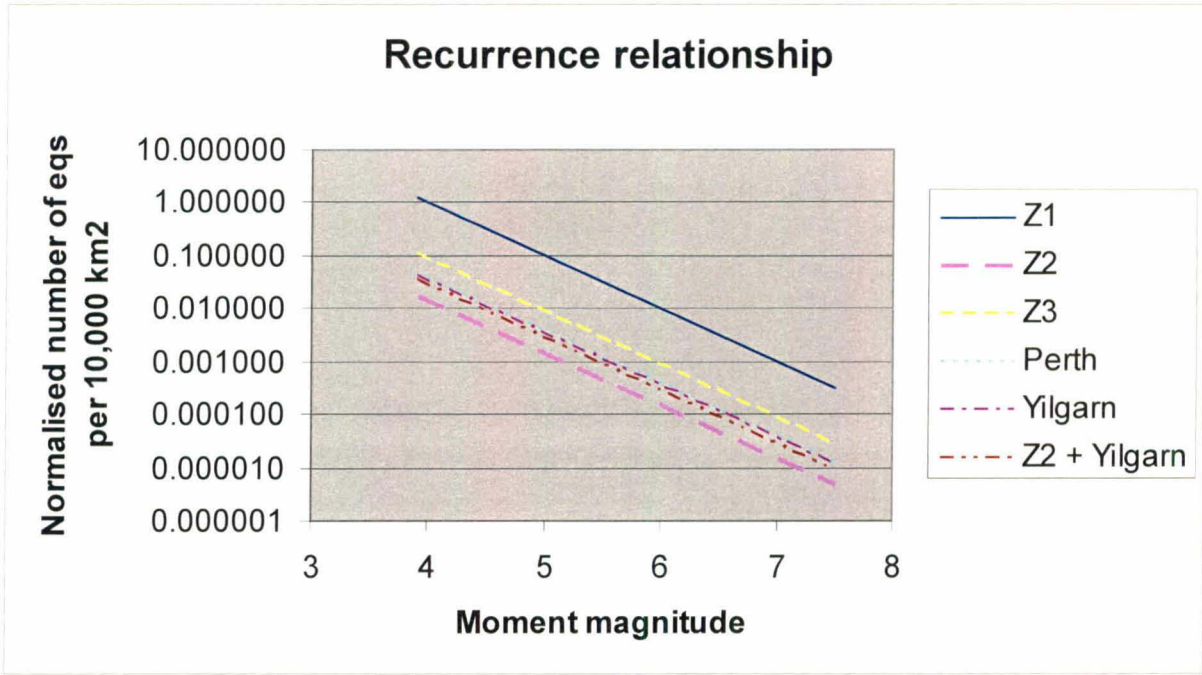

Figure 8: Recurrence relationship for the areal seismic zones

PRELIMINARY RESULTS AND REMARKS

For depicting earthquake ground motion severity, the predictive empirical relationship for intensity, peak ground acceleration (PGA) and spectral amplitudes at typical periods used in the Building Code (between 0.3 and 1.0 second) and for different site classes need to be considered. For this paper only the first-pass results for PGA on rock corresponding to 10% probability of exceedence in 50 years will be compared.

The current earthquake hazard model map of Australia is the 1993 AS 1170.4 acceleration coefficient map (Fig. 9) with 10% chance of exceedence in 50 years period. The acceleration coefficient is considered equal to PGA.

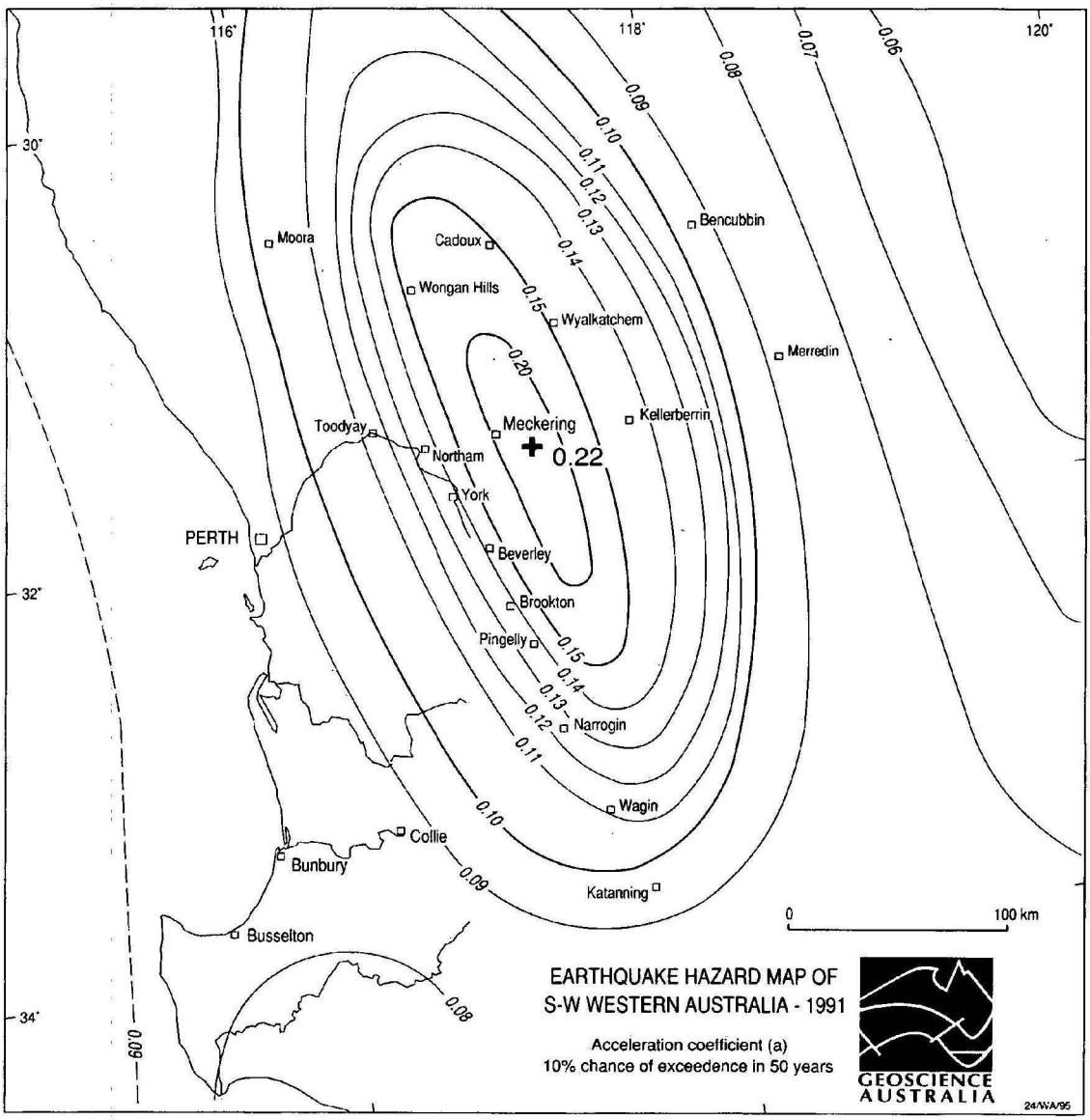

Figure 9: Earthquake hazard map of Western Australia

The results in terms of acceleration for the Perth region using our preferred zone definitions and Toro *et al.* (1997) attenuation relationship with seismological data up to 1st of July 2002 are presented in Figures 10, 11 and 12. The figures were produced with the variability option switched on and showed on average 50% higher values than when in the hazard program that option was switched off. The colour legend is individually adjusted and varies from picture to picture. For comparison, results using the Gaull *et al.* (1990) attenuation function are presented on the bottom.

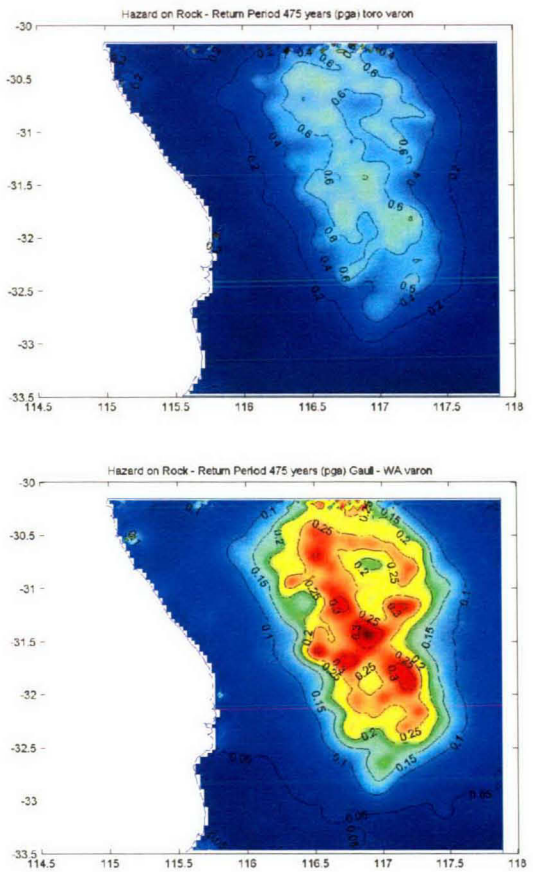

Figure 10: Peak ground acceleration for the Perth region (Model-I, Option-I, M_{max} of 7.5)

The differences between the simulations, Figures 10, 11 and 12, are mainly the result of a difference in the level of the mean and the variability associated with the Gaull *et al.* (1990) and Toro *et al.* (1997) attenuation functions. That is, Toro *et al.* formula predicts a slightly higher mean values and a larger variability with its estimates of ground motion. Gaull (pers. discussion, 2002) has indicated that the uncertainty in the Gaull *et al.* (1990) formula has been under estimated.

The different acceleration values between Fig. 9 and Figures 10, 11 and 12 could be the result of a method obtained to produce them (intensity in case of the Australian Standard) and our program selection. We have tested our program with variation of the Gutenberg-Richter *a* coefficient, the choice of attenuation function and its associated variability, and the range of maximum magnitude in the zones.

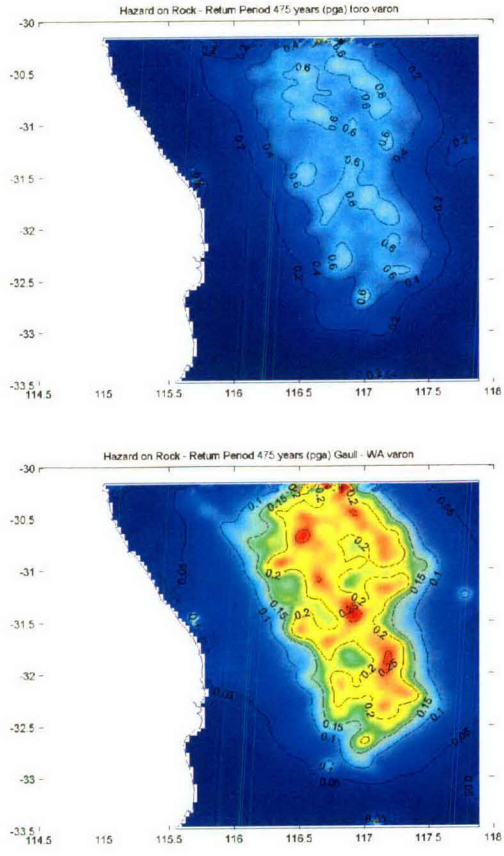

Figure 11: Acceleration coefficients for the Perth region using Model-I Option-II (M_{max} 7-8)

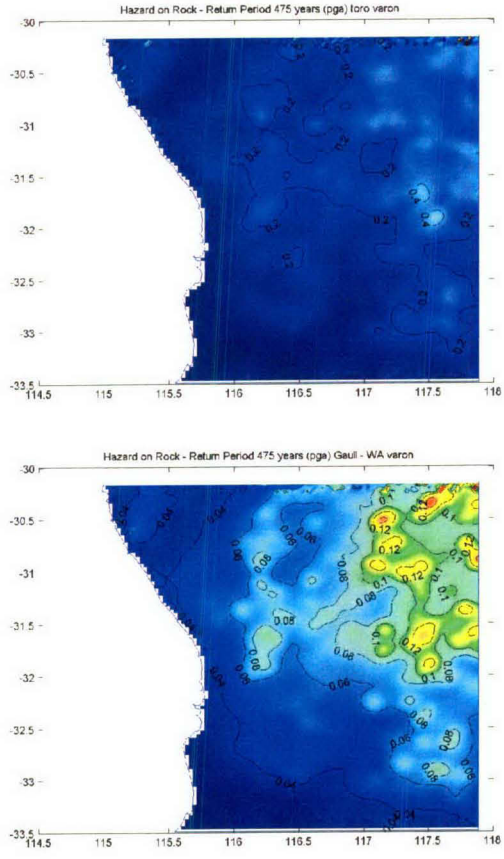

Figure 12: Acceleration coefficients for the Perth region using Model-II

No substantial difference was found between the PGA results when maximum moment magnitude of 7.5 or 8 was applied, as that would affect only the longer return periods. Model-II results however were influenced by the cell positioning and produced artefacts associated with discretisation process.

CONCLUSIONS

Our study identified the major geological and seismological components in the Perth region which might influence seismicity model and its parameters for Southwest Seismic Zone. Their optimisation and sensitivity analysis might be subject to further work in the hazard modelling process which will occur in the Cities Project Perth.

New evidence was presented that relates the spatial occurrence of earthquakes in the SWSZ to geological structures inferred by gravity and magnetic anomalies. The group of experts agreed upon the shapes of the seismic zones that are not significantly different from those proposed by Gaull *et al.* in 1990. With this revised configuration, the inclusion of 14 years of new seismic data indicates that seismicity in Zone 1 (corresponding to the SWSZ) is increased notably over previous estimates for that zone. This result has implications for the earthquake risk of communities in that zone or nearby. The new estimates of the seismicity in Zone 2 are lower than previous estimates.

The net effects of these new results on estimates of the earthquake hazard and risk in metropolitan Perth are yet to be determined. They will depend on several factors including the choice of attenuation function.

REFERENCES

Everingham, I.B., 1968. Seismicity of Western Australia. BMR report 132.

Everingham, I.B. and Gregson, P.J., 1970. Meckering Earthquake intensities and notes on earthquake risk for Western Australia. Bur. Miner. Resour. Aust. Rec. 1970/97.

Electric Power Research Institute, EPRI, 1993. Guidelines for Determining Design Basis Ground Motions, Vol. 5: Qantification of Seismic Source Effects.

Electric Power Research Institute, EPRI, 1994. The Earthquakes of Stable Continental Regions, Vol. 1: Assessment of Large Earthquake Potential.

Gaull, B.A., Kagami, H., Taniguchi, H., Gregson, P.J., Woad, G. and Page, B., 1991. The microzonation of Perth, Western Australia, using microtremor spectral ratios Bur. Miner. Resour. Aust. (unpublished).

Gaull, B.A., Michael-Leiba, M.O. & Rynn, J.M.W., 1990. Probabilistic earthquake risk maps of Australia. Australian Journal of Earth Sciences, 37, 169-187.

Gaull, B.A., Kagami, H., and Taniguchi, H., 1995. The microzonation of Perth, Western Australia, using microtremor spectral ratios. Earthquake Spectra, 11, 2, 173-191.

Gee, R.D., Baxter, J.L., Wilde, S.A. and Williams, I.R., 1981. Crustal development in the Archaean Yilgarn Block, Western Australia, Special Publications, Geological Society of Australia 7, 43-56.

Gordon F.R., 1994. The geological setting of intraplate earthquakes in Western Australia. Geological Society of Australia, Abstracts No. 37, p137-8. 12th Australian Geological Convention, Perth. September, 1994.

Gutenberg, B. and Richter, C.F., 1949. Seismicity of the Earth and associated phenomena, Princeton Univ. press.

Kárník, V., 1971. Seismicity of European Area - Part 2, D. Reidel Publishing Company, Dordrecht, Holland.

Mathur, S.P., 1976. Relation of Bouguer anomalies to crustal structure in southwestern and central Australia. BMR Journal of Australian Geology and Geophysics, 1, 277-286.

Myers, J.S., and Hocking, R.M. (compilers), 1998. Geological map of Western Australia, Geological Survey of Western Australia.

Sinadinovski, C., 2000, Computation of recurrence relation for Australian earthquakes, AEES conference, Hobart.

Toro, G.R., Abrahamson, N.A., and Schneider, J.F., 1997. Model of Strong Ground Motions from Earthquakes in central and Eastern North America: Best estimates and Uncertainties, Seismological Research Letters, 68, 41-57.

Utsu, T., 1999. Representation and Analysis of the Earthquake Size Distribution: A Historical Review and Some New Approaches, Pure and Applied Geophysics.

Walker G., 1998. Perth Earthquake Risk – has it been Over Rated? In Meckering, 30 years on – how would we cope today? AEES Proceedings of the 1998 Conference, Perth, Western Australia.

Weichert, D.H., 1980. Estimation of the earthquake recurrence parameters for unequal observation periods for different magnitudes, Bull. of the Seism. Soc. of America, v. 70.

Whitaker, A.J., 1992. Integrated geological and geophysical mapping of southwestern Western Australia. AGSO Journal of Australian Geology and Geophysics, 15, 313-328.

Whitaker, A.J., and Bastrakova, I.V., 2002. Yilgarn Craton aeromagnetic interpretation (1:1 500 000 scale map). Geoscience Australia.

Wilde, S.A., Middleton, M.F., and Evans, B.J., 1996. Terrane accretion in the southwest Yilgarn Craton: evidence from a deep seismic crustal profile. Precambrian Research, 78, 179-196.

APPENDIX A: HISTORICAL SEISMICITY

Edited by Cvetan Sinadinovski

According to the GA database 19 earthquakes with local magnitude 5 or more had occurred since 1945 in an area of 200 km around Perth. They are listed in Table A1.

Table A1: List of earthquakes with M≥5 in an area with radius of 200 km around Perth

Date	UTC	Lat	Long	Depth	Mag
19460419	211300	-33.5	114.5	0	5.7
19490502	100000	-30.9	116.4	0	5.1
19520311	60900	-31.3	116.5	0	5.1
19550829	60900	-30.7	116.4	0	5.3
19550830	135200	-30.7	116.4	0	5.8
19681014	25850.6	-31.62	116.98	10	6.9
19681015	33007	-31.68	117.03	10	5.7
19700310	171511.2	-31.11	116.47	1	5.9
19790601	215401.1	-30.812	117.177	6	5.2
19790602	94759.3	-30.827	117.179	3	6.2
19790603	74534.5	-30.77	117.17	10	5.3
19790607	64514.7	-30.8	117.179	6	5.5
19801208	001207.8	-32.12	114.11	37	5.2
19801210	43505.6	-30.73	117.15	13	5
19900117	63808.2	-31.72	116.99	6	5.5
20010928	25456.6	-30.489	117.054	2	5
20020305	14739	-30.489	117.102	2	5.1
20020323	131622.7	-30.524	117.091	5	5.1
20020330	211546.5	-30.533	117.109	5	5.2

The 1968 Meckering earthquake with magnitude M_L 6.9 was the strongest event and was felt within a radius of about 700 km (Everingham and Gregson, 1970). Intensities in the range MM VII to MM IX were observed within 14 km of the earthquake fault trace (Fig. A1-a and A1-b).

The isoseismal map enclosing the area of MM VI intensity was elongated to the east, indicating that damaging energy was best propagated in that direction (Everingham and Gregson, 1970). That effect probably decreased damage to Perth considerably (Fig. A1-c). A comparison of the isoseismal contours of the Meeberrie (1941) and Meckering earthquakes revealed that the Meeberrie magnitude was previously underestimated because the focal depth was probably greater than assumed and a local magnitude of 7.2 was determined from the isoseismals.

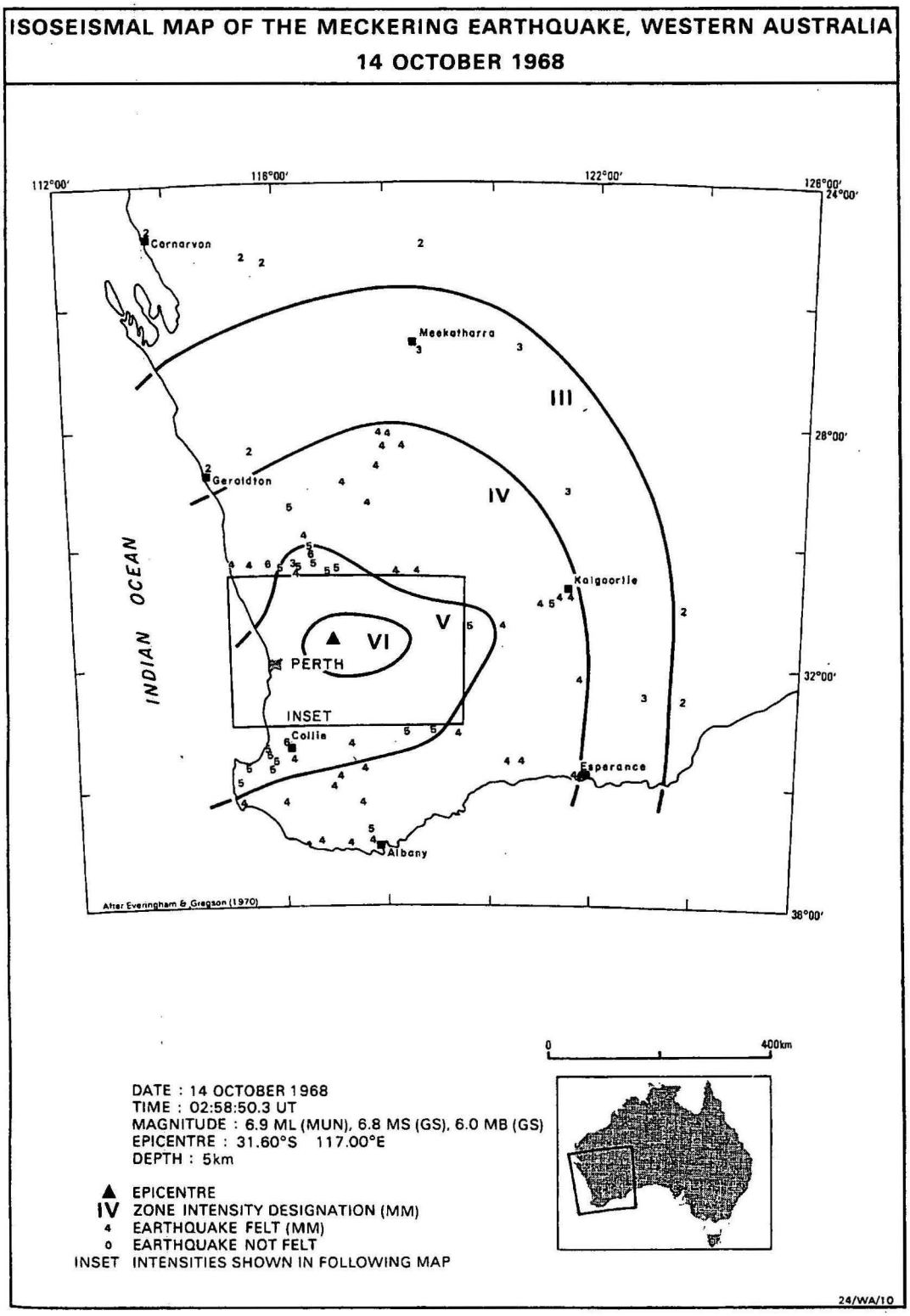

Figure A1-a: Isoseismal map of the Meckering earthquake, WA, 14th of October 1968

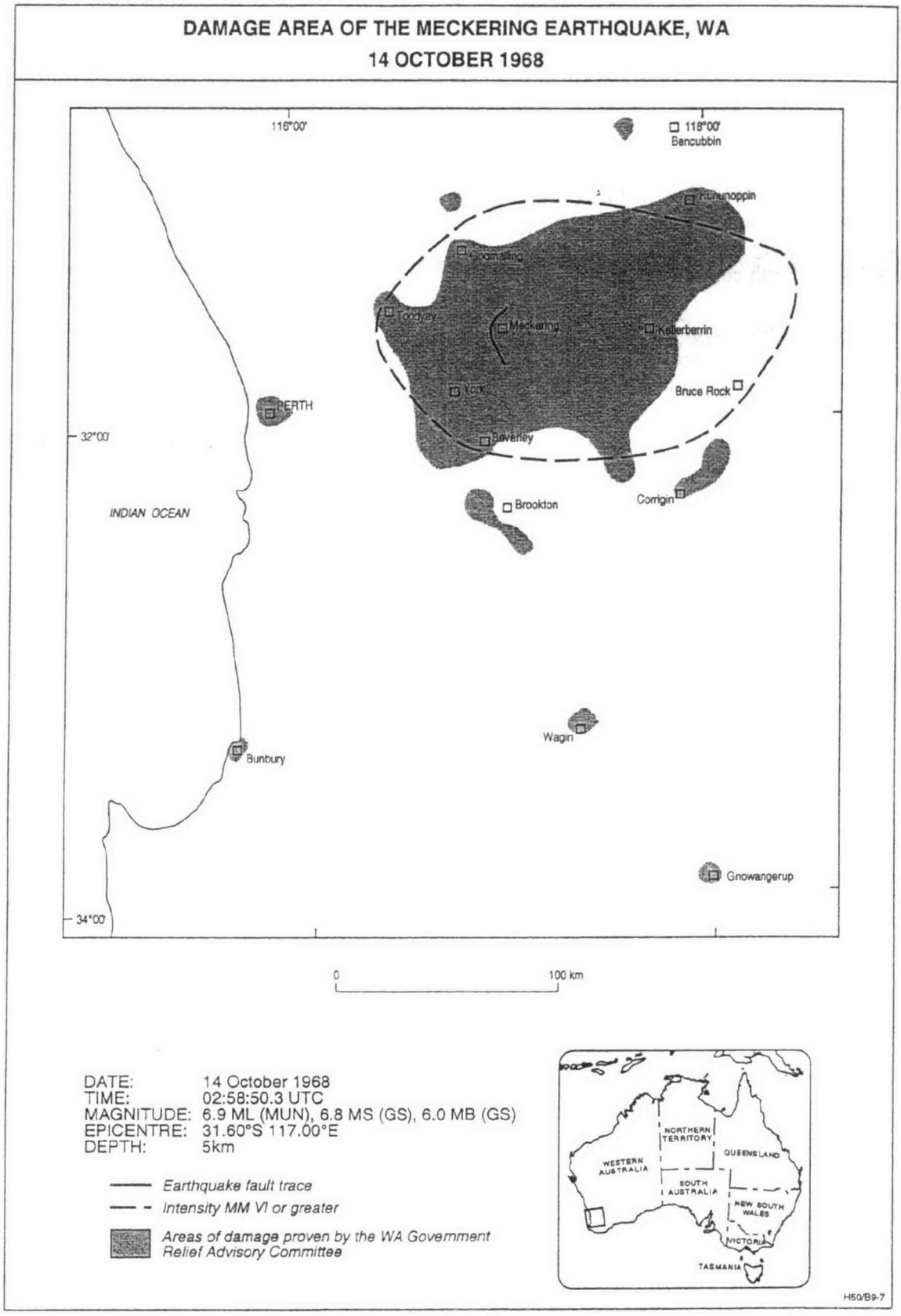

Figure A1-b: Damage area of the Meckering earthquake, WA, 14th of October 1968

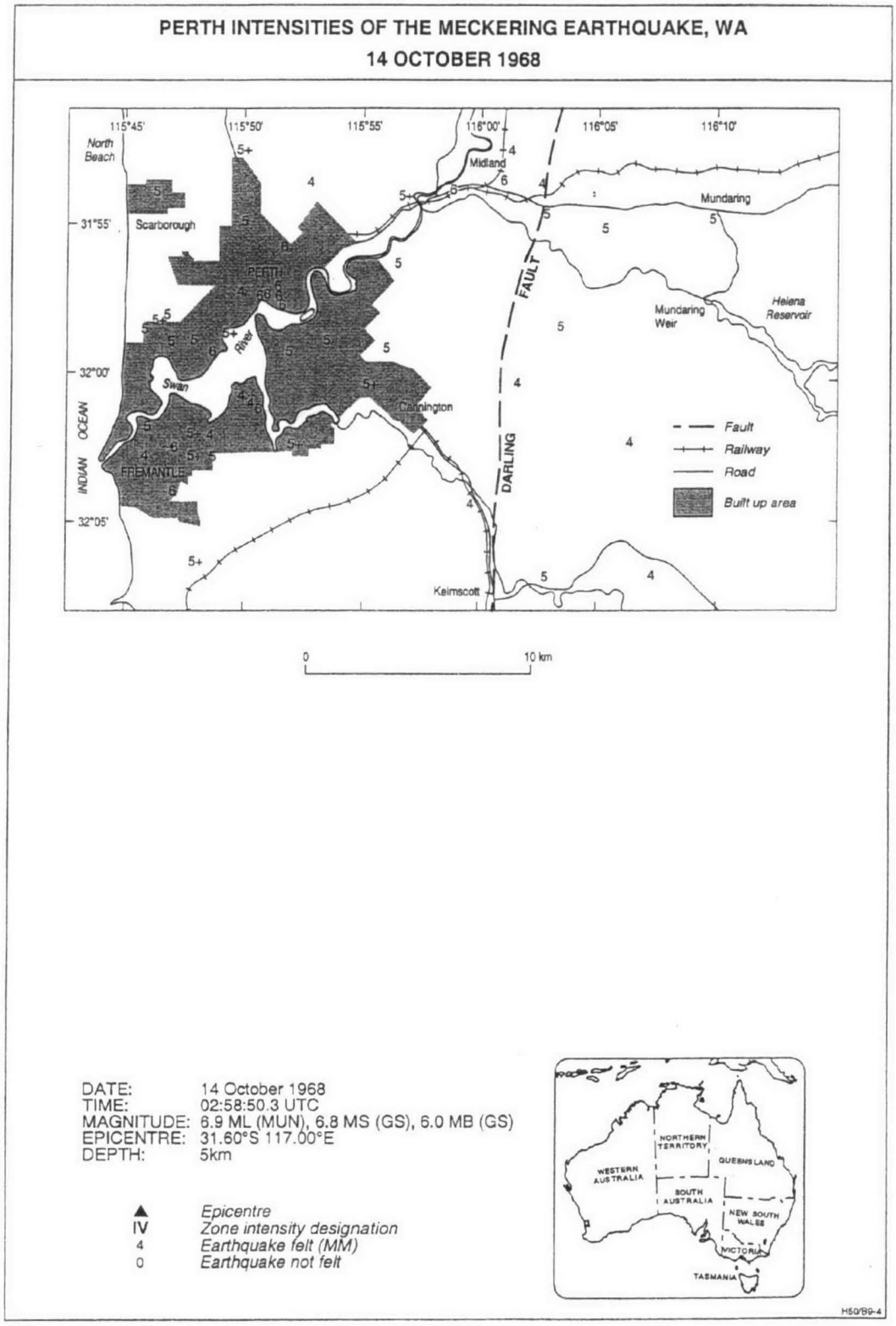

Figure A1-c: Perth intensities of the Meckering earthquake, WA, 14th of October 1968

The combined isoseismal and seismicity data showed that statistically Perth and central wheatbelt towns could suffer earthquake intensities of MM VII or more on an average of every few hundred years.

Empirical data for Perth areas underlain by thick unconsolidated earth (east of the city) showed that intensities were one unit higher for an unconsolidated area than for the shield area, at a given distance from an earthquake.

The focal mechanism of the Meckering Earthquake may support Everingham and Gregson (1970) suggestion that the seismic energy was transmitted more favourably towards the east. But because there was no actual instrumental data available, this premise is debatable. Gaull *et al.* (1995) state that the intensities for downtown Perth (as collected by Everingham and Gregson, 1970) were about one unit greater than that predicted by the attenuation function used in Gaull *et al.* (1990).

Furthermore, Figures A1-b and A1-c show that the areas of damage included Perth and not that immediately to the east of the Darling Fault. Downtown Perth intensities were at least MMVI whereas the maximum intensity to the east of the scarp was MMV even though this latter region was about 20% closer to the epicentre (Gaull *et al.*, 1995). There is also plenty of other information presented in this paper that shows the Perth Basin amplifies seismic energy, not the reverse. Finally, the late Ian Everingham agreed that his assigned intensities in downtown Perth might have been slightly underestimated (Gaull *et al.*, 1991).

The next largest event magnitude M 6.2 occurred at 17:48 local time on 2 June 1979 in the proximity of the small township of Cadoux in a farming area 180 km northwest of Perth. Cadoux was wrecked but only one person was injured (Gregson, 1980). The earthquake damaged or wrecked buildings and structures in an area of approximately 4000 km^2 centred on Cadoux. Roads, pipes, and power and railway lines were damaged by movements on a complex pattern of surface faulting caused by the earthquake in a zone extending 7 km to the north and to the south of Cadoux.

The isoseismal lines showed that the earthquake was felt clearly over a radius of 500 km (Fig. A2). The maximum Modified Mercalli intensity of MM IX was observed adjacent to the earthquake fracture, and intensities MM VII or greater occurred up to 5 km from the surface fracture. Intensities in Perth ranged between MM IV and MM V. Information from insurance and Government Works Department sources indicate that damage costs amounted to around $3.8 million (1979 prices).

Four accelerographs in the Meckering area, 90 km from Cadoux, recorded maximum accelerations of approximately 0.1 m/s^2. At Mundaring Weir, 120 km from Cadoux, the accelerograph recorded maximum east, vertical, and north component accelerations of 0.4, 0.2, and 0.1 m/s^2 respectively.

Members of the Mundaring Geophysical Observatory visited the Cadoux area to inspect damage. The area of damaging intensities of MM VII or more is about 300 km^2 and centred to the west of the earthquake's fault trace. The earthquake's fault plane determination indicates that the area of maximum intensity is possible on the surface projection of an east-dipping fault at depth, which contains the hypocentre, and that the surface faulting is subsidiary to this deeper faulting.

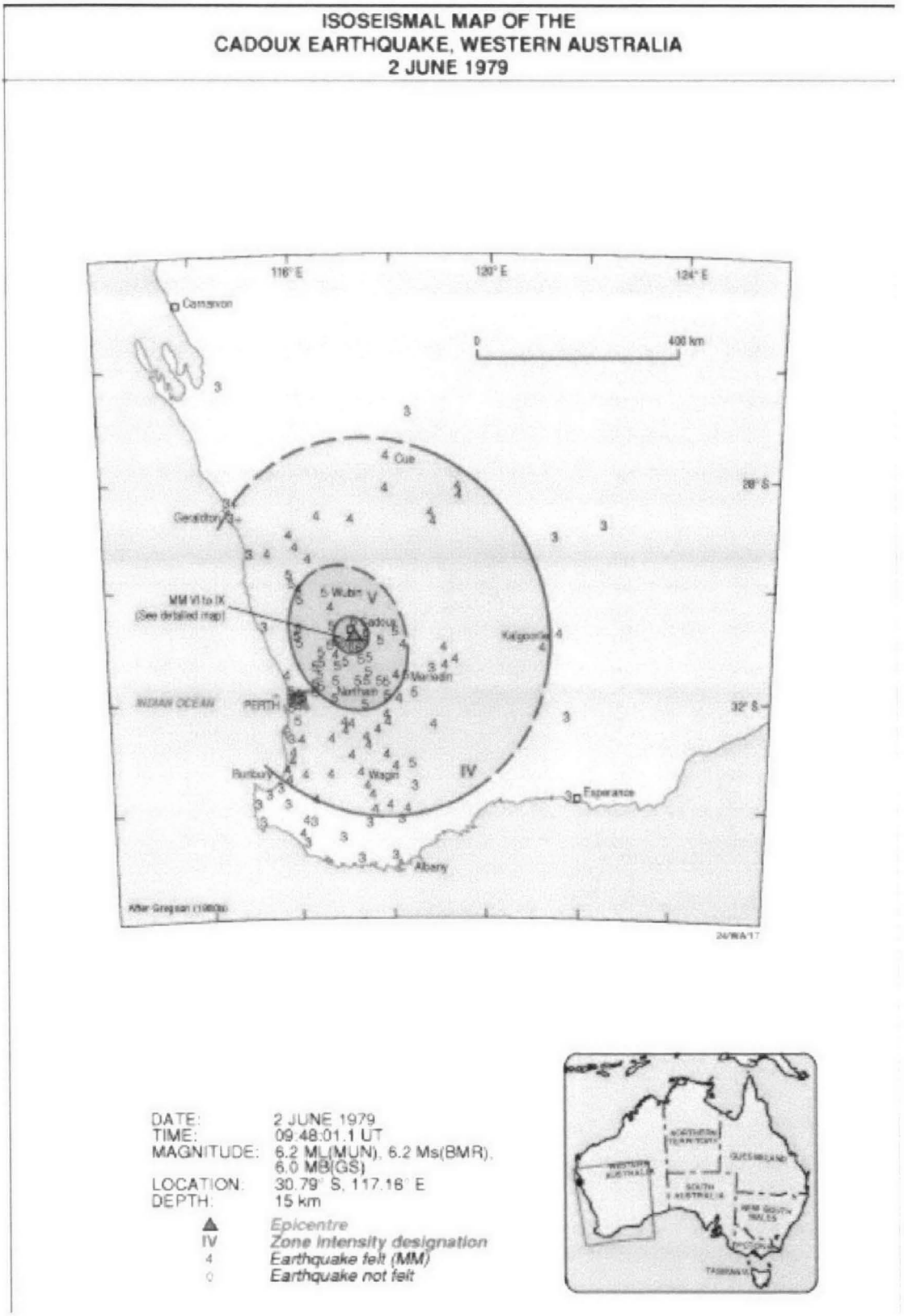

Figure A2: Isoseismal map of the Cadoux earthquake, WA, 2nd of June 1979

The other strong events include the Gabalong earthquake in 1955, the Calingiri earthquake in 1970, the offshore event in 1980 and the Burakin events in 2001 and 2002.

The isoseismal map of the Gabalong earthquake (Fig. A3) magnitude M 5.8 was drawn by staff of BMR's Mundaring Geophysical Observatory using newspaper reports and felt reports collected by the Perth Observatory (Everingham and Tilbury, 1972).

The isoseismal map of the Calingiri earthquake magnitude 5.7 is shown on Figure A4. Three hundred and sixty replies were received from about 420 questionnaires circulated within a 300 km radius of the earthquake epicentre. Although the earthquake caused an arcuate shallow east-dipping thrust fault over a distance of about 5 km, where the surface was uplifted by as much as 30 cm, major damage to buildings did not occur at Calingiri only 3 km from the fault.

No building straddled the fault, where the only damage was the shortening and misalignment of wire fences and a bump in a road where the fault scarp crossed it. Here it should be noted that the authors' rating of intensity (MM VI) is based largely on cracking of walls, in older homes, which because of their age, were considered to be in the "Masonry D" group as defined by Richter. However, G. A. Eiby (DSIR, NZ, personal communication) considered that, because the local standard of buildings was generally higher than in areas described by Richter, these types of building could be classified as "Masonry C", and that accordingly the authors' rating would tend to be too low (Everingham and Parkes, 1971).

A comprehensive description of the Calingiri earthquake is given by Gordon and Lewis (1980).

The isoseismal map of the offshore earthquake in 1980 is shown on Figure A5. The earthquake was located 150 km west of Fremantle and had a magnitude M_L 5.2. The maximum intensity reported was MM V at Fremantle and Cape Naturaliste. Felt intensities in the Perth region were generally higher to the east of the Darling Fault even though the earthquake was to the west of the fault. The earthquake was felt up to 350 km from the epicentre (Gregson, 1982).

The isoseismal map of the Burakin earthquake magnitude 5.1 in 2001 compiled by Cvetan Sinadinovski is shown on Figure A6. The earthquake occurred at 10:55 local time, 28 September and, being clearly felt in the wheat belt region, received wide publicity on radio and TV stations. The epicentre was about 15 km west of Burakin, some 190 km northeast of Perth. About 100 GA earthquake intensity questionnaires were issued and about half of these were completed and returned.

GA staff visited the areas between Perth and Cadoux and deployed instruments to record the aftershocks. Additional data from the questionnaire e-mailed to GA's web site were used to draw the isoseismal map.

The earthquake was felt at distances up to 190 km from the epicentre. The maximum intensity was MM V, too low to cause structural damage. Intensity in Perth was MM II and it was mainly felt on the top two floors of a six storey building in the central business area.

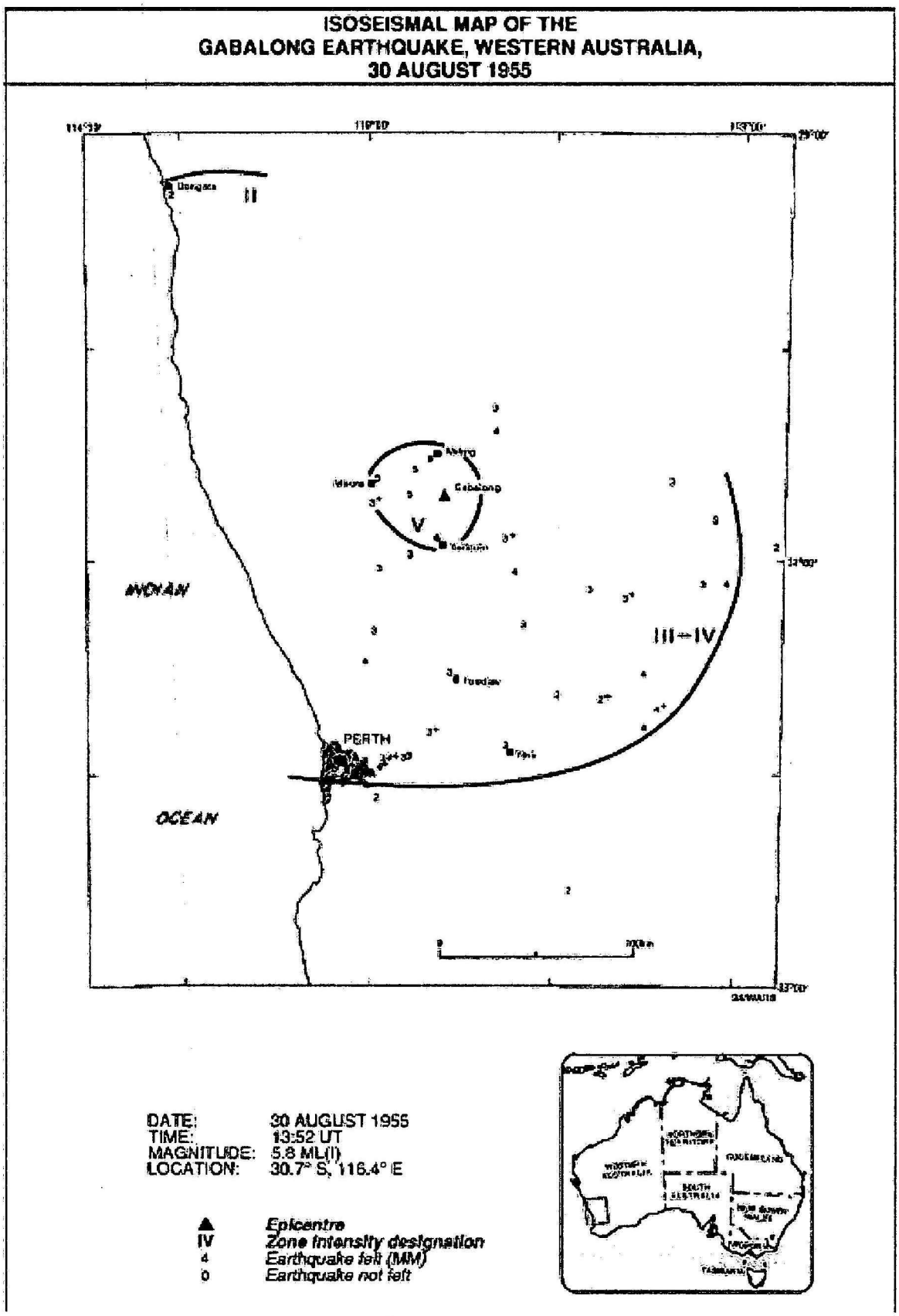

Figure A3: Isoseismal map of the Gabalong earthquake, WA, 30th of August 1955

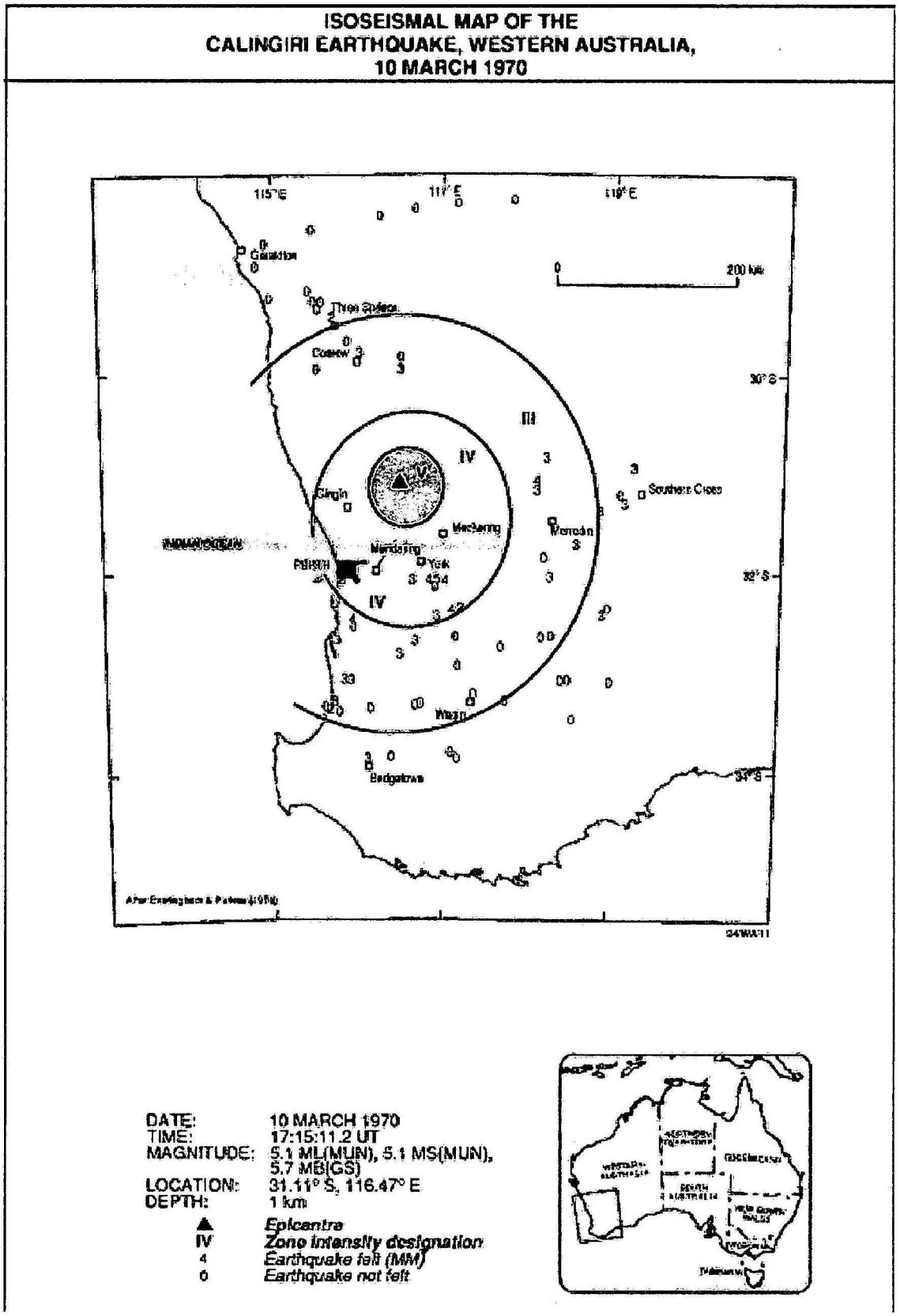

Figure A4: Isoseismal map of the Calingiri earthquake, WA, 10th of March 1970

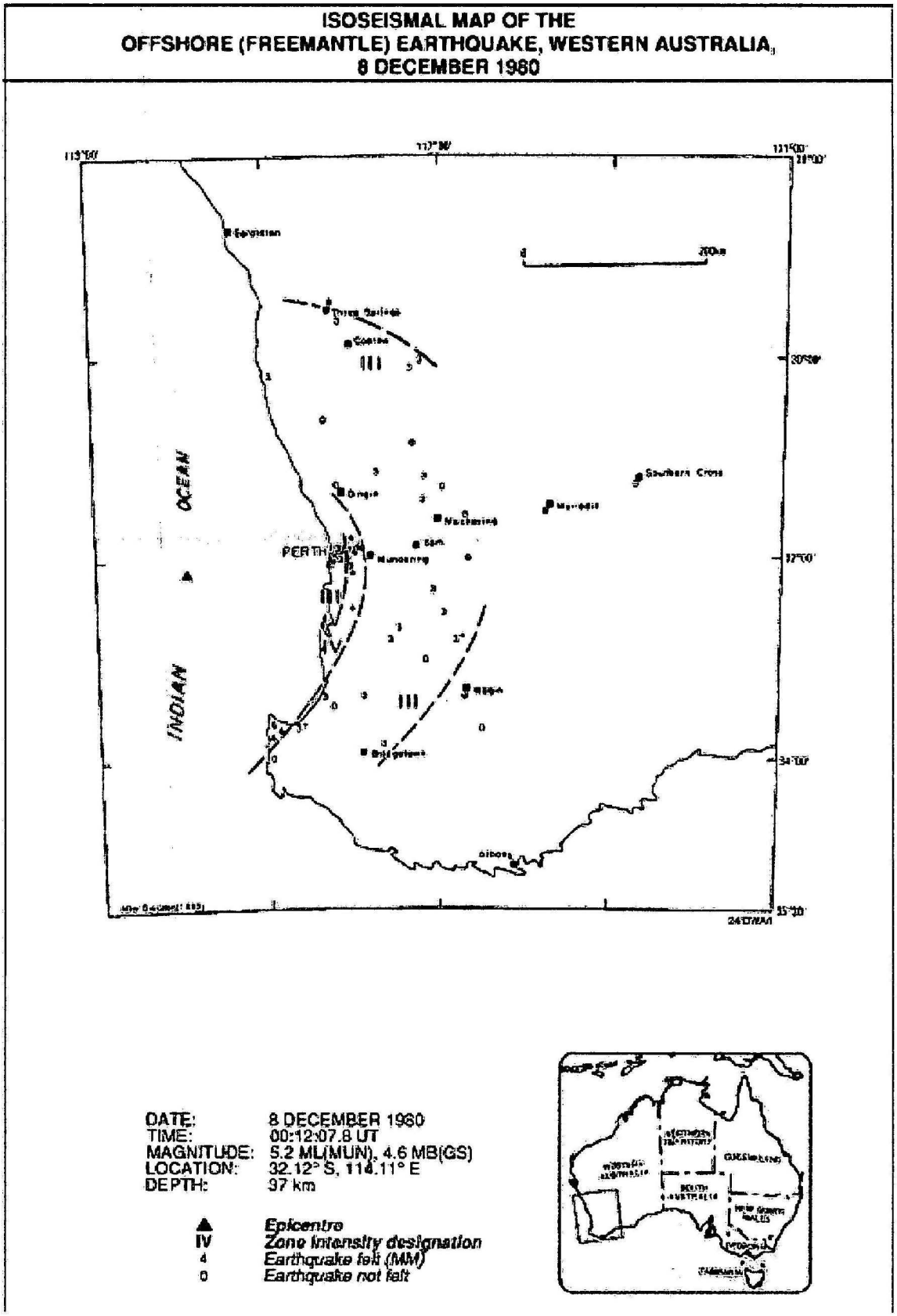

Figure A5: Isoseismal map of the offshore earthquake, WA, 8th of December 1980

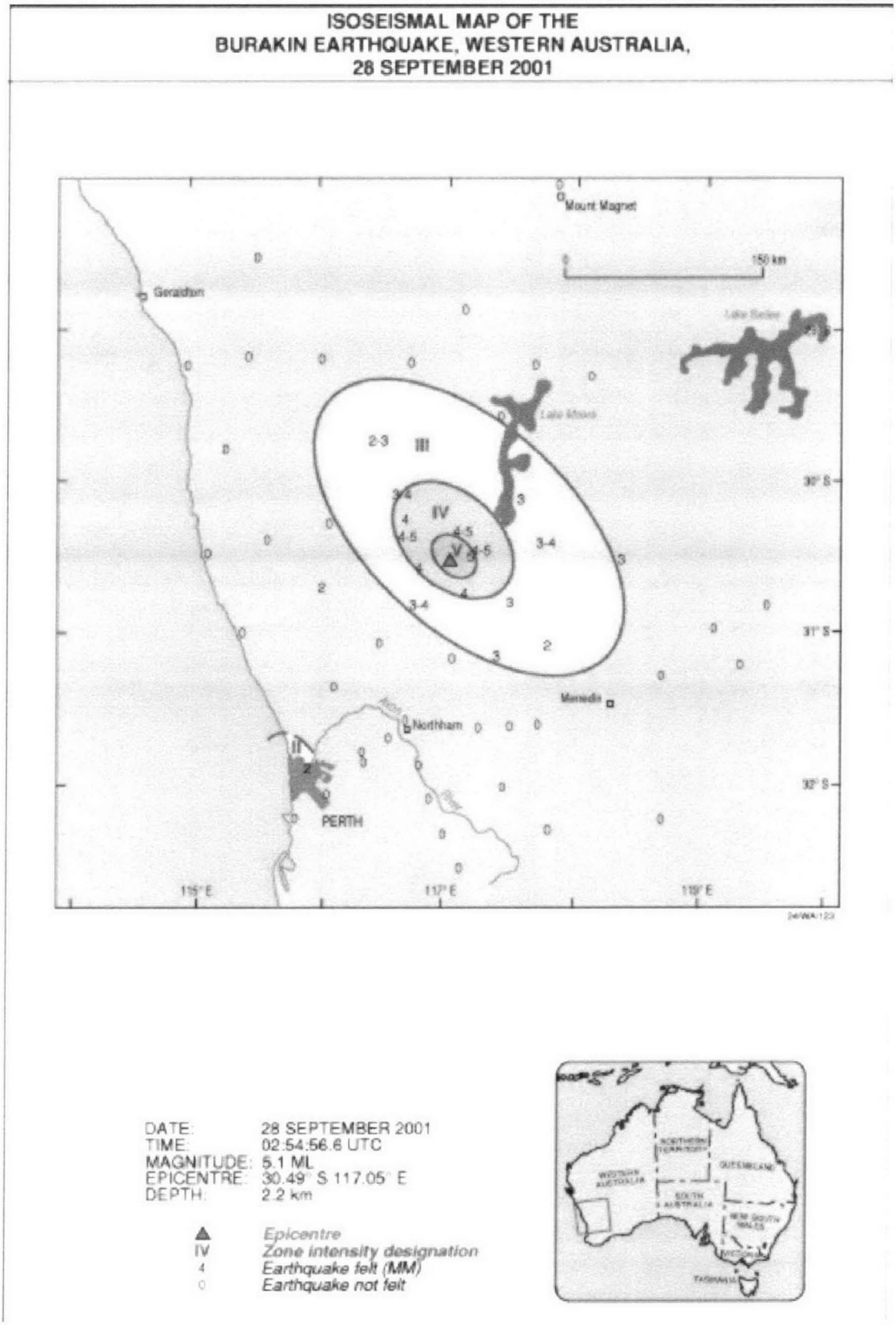

Figure A6: Isoseismal map of the Burakin earthquake, WA, 28th of September 2001

REFERENCES

Gaull B.A., Michael-Leiba M.O. and Rynn J.M.W., 1990. Probabilistic earthquake risk maps of Australia. Australian Journal of Earth Sciences, 37, 169-187.

Gaull B.A., Kagami H, Taniguchi H, Gregson P.J. Woad G. and Page B., 1991. The microzonation of Perth, Western Australia, using microtremor spectral ratios Bur. Miner. Resour. Aust. (unpublished).

Gaull B.A., Kagami H. and Taniguchi H., 1995. The microzonation of Perth, Western Australia, using microtremor spectral ratios. Earthquake Spectra, 11, 2, 173-191.

Gordon, F. R., and Lewis, J. D., 1980. The Meckering and Calingiri earthquakes, October 1968 and March 1970. Geological Survey of Western Australia, Bulletin 126.

Gregson, P. J., 1980. Mundaring Geophysical Observatory Annual Report, 1979. Bureau of Mineral Resources, Australia, Record 1980/51).

Gregson, P. J., 1982. Mundaring Geophysical Observatory Annual Report, 1980. Bureau of Mineral Resources, Australia, Record 1982/9 (unpublished).

Everingham, I.B., and Gregson, P.J., 1970. Meckering earthquake intensities and notes on earthquake risk in Western Australia. Bureau of Mineral resources, Australia, Record 1970/97.

Everingham, I. B., and Parkes, A. A., 1971. Intensity data for earthquakes at Landor (17 June 1969) and Calingiri (10 March 1970) and their relationship to previous Western Australian earthquakes. Bureau of Mineral Resources, Australia, Record 1971/80 (unpublished) .

Everingham, I. B., and Tilbury, L., 1972. Information on Western Australian earthquakes 1849-1960. Journal of the Royal Society of Western Australia, 55 (3), 90-96.

APPENDIX B: EARTHQUAKE FAULT PLANE SOLUTIONS

Compiled by Mark Leonard, Ian D. Ripper, and Li Yue

Australian continental earthquake fault plane solutions are listed and rated for reliability (Mark Leonard, Ian D. Ripper, and Li Yue, 2002, Australian earthquake fault plane solutions, GA report 19/2002). The earthquakes are also rated in terms of Australian Stress Map suitability as indications of the causative stress fields within the Australian continent (Zoback, 1992). Centroid moment tensor solutions such as those computed by the Harvard University Seismic Group are also given for comparison.

Apart from the centroid moment tensor solutions, the usual method has been to plot the seismic station P wave polarities, short and long period, on a stereographic projection of the lower focal hemisphere, Wulff or Schmidt projection. The regions of P wave positive and negative polarities are separated into quadrants by two mutually orthogonal nodal planes, one of which represents the fault plane. Selection of the fault plane is not usually possible, but may be influenced by such factors as surface rupture or aftershock pattern.

The orientations of the Pressure (P) and Tension (T) axes of the earthquake solution are interpreted as giving an indication of the orientations of the maximum and minimum principal stress axes of the causative tectonic stress field. However this coincidence may not occur, for example, if the earthquake occurred on a pre-existing fault.

Interpretations in terms of compressive stress should distinguish between (a) a horizontal P axis being evidence for compressive stress as well as giving the orientation, and (b) a compressive stress is already determined by some other means, and the P axis merely gives an indication of its orientation. Also, Australian earthquake solutions may have been over-interpreted in terms of a compressive causative tectonic stress field by assuming a compressive cause if the P axis of the solution plunges at an angle less than about 45° from the horizontal. A horizontal T axis, such as occurs in a strikeslip solution where both P and T axes are approximately horizontal, is generally ignored. A strikeslip earthquake may also be caused by a tensional stress, or a simple shear, in which the acting force is parallel to the fault plane.

Interpretations of the fault plane solutions besides a compressive causative stress field should not be discarded. The existence of quaternary volcanism in some parts of Australia could, for example, indicate the existence of a tensional tectonic stress field component.

Meckering, 14th October

Date :1968 October 14
Place :Meckering,WA., Perth and Kellerberrin 1:250000 maps.
Surface expression :Everingham(1968) reported that fracturing of the Earth's crust had occurred along an arc 32 km long, which trended roughly north-south with its convex side to the west. At the fracture zone a distinct scarp was formed by the movement of the eastern side upwards by up to 1.5 metres. A crustal shortening of up to 2 metres was also evident at the fracture zone, and the east block moved south by up to 0.9 metres relative to the area west of the fracture. --- The effects at the surface are believed to be due to shallow thrust faulting with a right hand (dextral) strikeslip component. The fault plane has an apparent east dip of about

35° judging by the ground displacements. --- Aftershocks occurred, most within about 8 km of the trace of the fracture zone and to the east of it.

Solution Reference :Fredrich *et al.*(1988).
Hypocentre source :ISC
Type of analysis :Moment tensor (Drawn on Schmidt Projection).
Magnitudes :MS 6.8; Seismic moment $10.40\pm0.53*10^{18}$newton metre
Origin time (UTC) :025851.8
Hypocentre, Latitude:-31.54 **Longitude**:117.00 **Depth(km)**:1-5
Mechanism :
Nodal plane 1, Strike:351±10 Dip:29±7 Slip:73±10 **Pole**, Azimuth:261 Plunge:61
Nodal plane 2, Strike:190 Dip:63 Slip:99 **Pole**, Azimuth:100 Plunge:27
T axis Azimuth:122 Plunge:71
N axis Azimuth:006 Plunge:09 **Uncertainty**:Moment tensor
P axis Azimuth:273 Plunge:17
Zoback Rating:C
Fault Plane Rating:3
Comments :Fredrich *et al.*(1988), found the best fitting mechanism to be almost pure thrust faulting on a north striking plane, with centroid depth 3 km. They took the east dipping plane to be the fault plane because of its agreement with surface rupture. Their uncertainty in strike, dip and slip angles of ±10°, ±7°, and ±10° respectively, and differences with Vogfjord and Langston(1987) values of 7°, 1°, and 5° respectively, endorse the '3' Fault Plane Rating given to Moment Tensor Solutions.

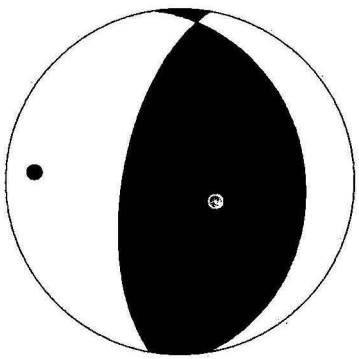

Solution Reference :Fitch *et al.*(1973)
Hypocentre source :Fitch *et al.(*1973)
Type of analysis :P wave polarity plus S wave polarization and displacement spectral densities computed from Rayleigh waves, Schmidt Projection.
Magnitudes :MS 6.8, seismic moment $6.1*10^{25}$ dyne cm.
Origin time (UTC) :025851
Hypocentre, Latitude:-31.68 **Longitude**:117.00 **Depth(km)**:15
Mechanism :Overthrust combined with sinistral strikeslip.
Nodal plane 1, Strike:332 Dip:68 Slip: **Pole**, Azimuth: Plunge:
Nodal plane 2, Strike:038 Dip:45 Slip: **Pole**, Azimuth: Plunge:
T axis Azimuth:020 Plunge:50
N axis Azimuth:169 Plunge:36 **Uncertainty**: Not rated
P axis Azimuth:271 Plunge:13

Zoback Rating:X
Fault Plane Rating:X
Comments :USCGS depth, 1 km. ISC depth, 18 km. This solution is not rated as it does not fit the surface data, a fact recognised in the reference. The earthquake is seen as a multiple rupture, starting about 3.5 seconds before the main shock, as a sinistral strike slip motion more or less consistent with the P wave data. But motion is envisaged to be on the plane striking NNW, dipping WSW, with overthrust and strike slip motions opposite to the surface expressions. The P wave data alone is inconsistent with the given overthrust solution on NNW strike, although additional information in the form of S wave polarisation data and displacement spectral density data computed from Rayleigh waves were used in the analysis.

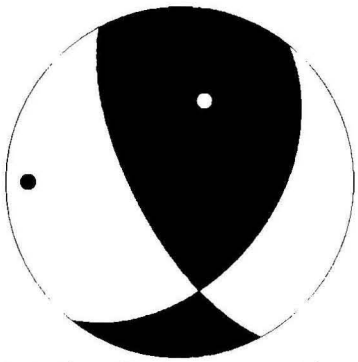

Solution Reference :The P wave data of Fitch *et al.*(1973), Figure 2, and page 350.
Hypocentre source :Fitch *et al.*(1973).
Type of analysis :P wave polarity, Schmidt Projection.
Magnitudes :MS 6.8
Origin time (UTC) :025851
Hypocentre, Latitude:-31.68 **Longitude**:117.00 **Depth(km)**:5
Mechanism :Dextral strikeslip
Nodal plane 1, Strike:019 Dip:82 Slip: **Pole**, Azimuth:289 Plunge:08
Nodal plane 2, Strike:109 Dip:82 Slip: **Pole**, Azimuth:019 Plunge:08
T axis Azimuth:335 Plunge:11
N axis Azimuth:151 Plunge:79 **Uncertainty**:Anomalous stations
P axis Azimuth:63 Plunge:01
Zoback Rating:X
Fault Plane Rating:X
Comments :Fitch *et al.*(1973) note that their P wave data, their Figure 2, are consistent with a strikeslip solution for an initial event 3.5 seconds before the main shock. The solution given here using the P wave polarity data and the position of the B (N) axis given on page 350, is a tight strikeslip solution, but dextral on a NNE trending plane rather than on the NNW trending plane. As Fitch *et al.*(1973) were not happy with the quality of some P wave data anyway, and as they used additional information to get their overthrust solution, this strike slip solution is not rated. An additional strikeslip solution has been drawn from the same data (Fitch *et al.*, 1973, Figure 2). The solution is tight with a couple of anomalous stations. The motion would be dextral on the plane striking NNE. The parameters are given below.

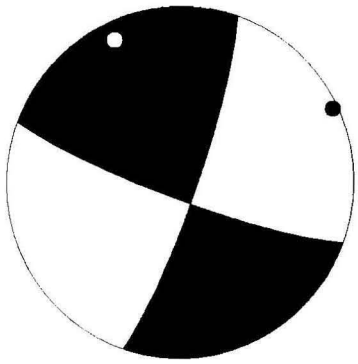

Solution Reference :Vogfjord and Langston(1987)
Hypocentre source :Vogfjord and Langston(1987)
Type of analysis :Moment tensor (shown on Schmidt Projection).
Magnitudes :MS 6.8, Seismic moment $8.2*10^{25}$ dyne cm
Origin time (UTC) :
Hypocentre, Latitude: **Longitude**: **Depth(km)**:3
Mechanism :Overthrust
Nodal plane 1, Strike:341 Dip:37 Slip:61 **Pole**, Azimuth:251 Plunge:54
Nodal plane 2, Strike:015 Dip:58 Slip:119 **Pole**, Azimuth:105 Plunge:31
T axis Azimuth:148 Plunge:69.9
N axis Azimuth:004.5 Plunge:16.7 **Uncertainty**:Moment tensor
P axis Azimuth:271 Plunge:11.3
Zoback Rating:C
Fault Plane Rating:3
Comments :Vogfjord and Langston(1987) indicate a depth of 3 km for the earthquake, rupture initiating at depth 1 km (1.5 km in Langston(1987)) and progressing radially (downward) to a depth of nearly 6 km. Their fault plane dips eastward at a shallow angle in agreement with the surface rupture. Langston(1987) stated that considering the size of the Meckering earthquake and the 37-km-long fault scarp that it produced, it is evident that this area is currently unique among the seismogenic regions of the Earth. The small foreshock 3.5 seconds before the main shock was not included in the "inversion window".

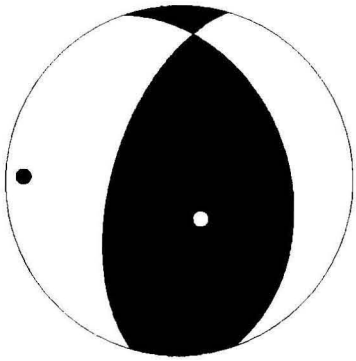

Further comments :Gordon and Wellman(1971), with revisions to the diagram by Gordon and Lewis(1980, Figure 74 page 162), offered a possible mechanism for the Meckering earthquake to produce a dextral fault component in a sinistral shear zone. They considered that the zone of earthquakes which strikes northwest across southwest Western Australia, the South-western Australian Seismic Zone, involves sinistral shear. They envisaged a spherical cap sitting on the shear zone and extending out beyond the shear zone on both sides, to the southwest and northeast. A slow buildup of elastic strain occurs in the part of the upper cap

within the shear zone. The section of cap outside the shear zone remains unstrained. The cap then snaps free from the underlying rock to resume its unstrained state. Gordon and Wellman(1971) and Gordon and Lewis(1980) assertted that this rebound involves dextral faulting at the margin of the cap. However their hypothesis appears to be in error in their very first stage, the straining of the cap before earthquake rebound. The figure (Figures 2 and 74 respectively), shows strain deformation (change of shape) in the sections of the cap outside the shear zone, as well as within, contrary to the statement "and the part outside is carried along bodily without being strained".

Denham *et al.*(1980) also discussed a possible earthquake trigger for the Meckering earthquake. They found the stress drop to be ~9Mpa. Measurements of maximum principal stress by shallow overcoring was highest, 23Mpa, at the site farthest north from the epicentre, and the lowest, 4Mpa, near the epicentre. As a cause of the earthquake, Denham *et al.*(1980) proposed that the fault plane is progressively weakened by alteration or weathering, and that a small long term fluctuation of head of groundwater was the trigger.

Cadoux, 2nd June 1979

Date :1979 June 02
Place :Cadoux, southwest Western Australia; Bencubbin 1:250000 Map.
Surface expression :Complex set of new surface faults within a north-south zone 15 km long and 3 km wide. Main movement in central part of zone was west over east, maximum throw about 1.3m with a dextral strike slip component (Denham *et al.*(1987). More detail is provided in Denham *et al.*(1987) and in Lewis (1981).

Solution Reference :Denham *et al.*(1987).
Hypocentre source :Denham *et al.*(1987).
Type of analysis :Long period P and SH wave inversion, and P wave polarities, Schmidt projection
Magnitudes :ML 6.2; mb 5.9; MS 6.0.
Origin time (UTC) :094758.7
Hypocentre, Latitude:-30.83 **Longitude**:117.18 **Depth(km)**:6
Mechanism :Overthrust
Nodal plane 1, Strike:165 Dip:26 Slip: **Pole**, Azimuth:075 Plunge:64
Nodal plane 2, Strike:007 Dip:64 Slip: **Pole**, Azimuth:277 Plunge:26
T axis Azimuth:299 Plunge:68
N axis Azimuth:182 Plunge:09 **Uncertainty**:Inversion.
P axis Azimuth:090 Plunge:18
Zoback Rating:C
Fault Plane Rating:3
Comments :The nodal plane data was not provided, but was measured off the projection. The nodal plane striking north-south and dipping to the west would be favoured as the fault plane to agree with mid-fault surface overthrust displacement, west side over east.

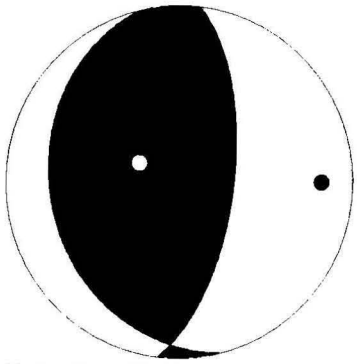

Solution Reference :Harvard University Seismology Group
Type of analysis :Centroid Moment Tensor
Zoback Rating:C
Fault Plane Rating:
060279A WESTERN AUSTRALIA**
Date (y/m/d): 1979/6/2
Information on data used in inversion

Wave	nsta	nrec	cutoff
Body	10	26	45
Mantle	4	7	135

Timing and location information

	hr	min	sec	lat	lon	depth	mb	Ms
MLI	9	47	58.10	-30.81	117.18	6.0	6.0	6.1
CMT	9	48	5.00	-30.86	116.99	15.0		
Error			0.30	0.03	0.03	-1.0		

Assumed half duration: 4.2
Mechanism information
Exponent for moment tensor: 25 units: dyne/cm

	Mrr	Mtt	Mpp	Mrt	Mrp	Mtp
CMT	1.280	0.380	-1.660	-0.810	0.090	0.250
Error	0.030	0.030	0.040	0.080	0.110	0.030

Mw = 6.1 Scalar Moment = 1.73e+25
Fault plane: strike=200 dip=49 slip=132
Fault plane: strike=326 dip=56 slip=52
Eigenvector: eigenvalue: 1.75 plunge: 59 azimuth: 178(T)
Eigenvector: eigenvalue: -0.05 plunge: 30 azimuth: 349(N)
Eigenvector: eigenvalue: -1.70 plunge: 4 azimuth: 82(P)
Comments :Although the Harvard CMT solution is an overthrust similar to the inversion solution of Denham *et al.*(1987), it is noted that the positions of the respective N axes differ by about 40°.

Station Name	Azimuth	Plunge	C + D -
	0	83	+
	4	51	+
	6	53	+
	13	59	+
	14	30	+
	14	43	+
	14	39	-

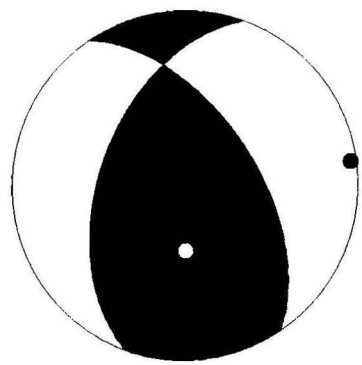

18	25	+
28	83	+
38	59	+
54	62	-
58	55	+
60	64	-
70	83	+
70	54	-
71	38	-
90	42	-
90	60	-
84	28	-
97	57	-
101	46	-
108	52	-
110	40	-
113	58	+
116	48	-
121	64	-
127	54	-
177	26	+
204	66	+

Burakin, September 28th 2001

Date : 28/09/2001
Place : Burakin, Western Australia
Surface expression : none
Solution Reference : Clark D.
Hypocentre source : GA
Type of analysis : First motion
Magnitudes : M_L 5.1
Origin time (UTC) : 0254 UT
Hypocentre, Latitude: -30.485 **Longitude**: 117.124 **Depth(km)**: 2.01
Mechanism : strike-slip
Nodal plane 1, Strike: 22 Dip: 61 Slip: -174 **Pole**, Azimuth: 112 Plunge: 29
Nodal plane 2, Strike: 289 Dip: 85 Slip: -31 **Pole**, Azimuth: 19 Plunge: 5
T axis Azimuth: 339 Plunge: 17
N axis Azimuth: 100 Plunge: 60 **Uncertainty**: Tight
P axis Azimuth: 241 Plunge: 24
Zoback Rating: A
Fault Plane Rating: 1
Comments : 18 stations
very tight fit
Station MEEK does not fit solution

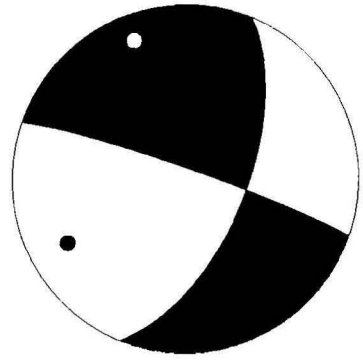

Station	Azimuth	Plunge	D/C
BLDU	247	4.1	-
KLBR	151	-30.8	+

MUN	205	-42.2	-
MORW	327	-42.2	+
MEEK	19	-42.2	-
RKGY	180	-42.2	-
KMBL	103	-42.2	+
GIRL	341	-42.2	-
FORT	94	-42.2	e
FITZ	34	-42.2	+
BBOO	103	-42.2	-
ASPA	69	-42.2	e
STKA	100	-55.4	e
ARPS	113	-56.2	+
KAKA	41	-57.4	+
QLP	87	-57.9	-
CMSA	99	-57.9	-
RMQ	89	-60.1	+

Burakin December 28th 2001

Date : 28/12/2001
Place : Burakin
Surface expression : none

Solution Reference : Clark D.
Hypocentre source : GA
Type of analysis : First motion
Magnitudes : M_L 4.5
Origin time (UTC) : 1631 UT
Hypocentre, Latitude: -30.565 **Longitude**: 117.052 **Depth(km)**: 2.19
Mechanism : thrust
Nodal plane 1, Strike: 282 Dip: 42 Slip: 76 **Pole**, Azimuth: 12 Plunge: 48
Nodal plane 2, Strike: 120 Dip: 50 Slip: 102 **Pole**, Azimuth: 210 Plunge: 40
T axis Azimuth: 088 Plunge: 80
N axis Azimuth: 293 Plunge: 9 **Uncertainty**: <20deg in azimuth, <5deg in dip
P axis Azimuth: 202 Plunge: 4
Zoback Rating: C
Fault Plane Rating: 3
Comments : 14 stations
very tight fit
Stations MUN and KAKA do not fit solution

Station	Azimuth	Plunge	D/C
BLDU	260	4.4	-
KLBR	149	-30.8	+
MUN	206	-30.8	+
MORW	329	-42.2	+
RKGY	180	-42.2	-
MEEK	19	-42.2	-
KMBL	102	-42.2	+
GIRL	341	-42.2	e

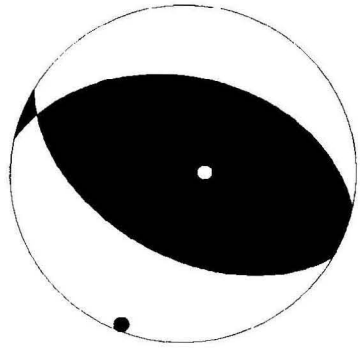

FORT	94	-42.2	e
FITZ	34	-42.2	+
BBOO	102	-42.2	e
ASPA	69	-42.2	+
STKA	99	-55.3	+
KAKA	41	-57.4	-

REFERENCES

Denham, D., Alexander, L.G., and Worotnicki, G., 1980. The stress field near the sites of the Meckering (1968) and Calingiri (1970) earthquakes, Western Australia. Tectonophysics, 67, 283-317.

Denham, D., Alexander, L.G., Everingham, I.B., Gregson, P.J., McCaffrey, R., and Enever, J.R., 1987. The 1979 Cadoux earthquake and intraplate stress in Western Australia. Australian Journal of Earth Sciences, 34, 507-521.

Everingham, I.B., 1968. Preliminary report on the 14 October 1968 earthquake at Meckering, Western Australia. Australia Bureau of Mineral Resources Record 1968/142.

Fitch, T.J., Worthington, M.H., and Everingham, I.B., 1973. Mechanisms of Australian earthquakes and contemporary stress in the Indian Ocean Plate. Earth and Planetary Science Letters, 18, 345-356.

Fredrich, J., McCaffrey, R., and Denham, D., 1988. Source parameters of seven large Australian earthquakes determined by body wave inversion. Geophysical Journal, 95, 1-13.

Gordon, F.R., and Lewis, J.D., 1980. The Meckering and Calingiri earthquakes October 1968 and March 1970. Geological Survey of Western Australia Bulletin 126.

Gordon, F.R., and Wellman, H.W., 1971. A mechanism for the Meckering earthquake. Recent Crustal Movements, Royal Society of New Zealand, Bulletin 9, 95-96.

Langston, C.A., 1987. Depth of faulting during the 1968 Meckering, Australia, earthquake sequence determined from waveform analysis of local seismograms. Journal of Geophysical Research, 92, 11561-11574.

Lewis, J.D., 1981. The Cadoux earthquake, June 1979. Western Australian Geological Survey Report, 11.

Vogfjord, K.S., and Langston, C.A., 1987. The Mechering earthquake of 14 October 1968: A possible downward propogating rupture. Bulletin of the Seismological Society of America, 77, 1558-1578.

Zoback, M. L., 1992. First- and second-order patterns of stress in the lithosphere: The World Stress Map Project. Journal of Geophysical Research, 97, 11703-11728.

APPENDIX C: EARTHQUAKE SOURCE CONFIGURATION
Brian Gaull, Marion Michael-Leiba and Jack Rynn – edited by Cvetan Sinadinovski

The original formation of the source zones was proposed by Gaull, Michael-Leiba and Rynn in "Probabilistic earthquake risk maps of Australia", published in the Australian Journal of Earth Sciences in 1990.

Such configuration of the source zones was chosen by:

- satisfying the requirements of their computer program for the zones to be made up of a series of quadrilaterals;
- the areal distribution of epicentres up to the end of 1986;
- using relevant geological and tectonic factors.

The WA zones as defined by Gaull *et al.* (1990) are shown on Fig. C1. The figure shown here represents epicentres for all the earthquakes till 2002 from the GA's catalogue with magnitudes equal to or greater than 2.5.

The most significant zones which will determine the seismic hazard in Perth are:

1) Meckering-Cadoux zone which is considered the highest hazard zone in WA and probably the most important due to its distance from the city of Perth. It contains the epicentres of the devastating 1968 Meckering M_L 6.9 and 1979 Cadoux M_L 6.2 earthquakes;
2) Southwest Seismic Zone with seismic activity between 30° and 35° South, and 116.5° to 118.5° East;
3) Southwestern continental shelf zone with considerable offshore activity and includes the largest earthquake known in Australia, 1906 magnitude M_L 7.4;

background zone of low seismicity beneath Perth and to a lesser extent:

4) Southwestern ocean zone along the 5000 m isobath;
5) Fraser Fault zone with seismic activity associated with the Fraser fault;
6) Kalgoorlie zone with activity mainly resulting from rock bursts in mines in the area;
7) Indonesian seismic zone with large distant earthquakes which might be felt in tall structures in Perth.

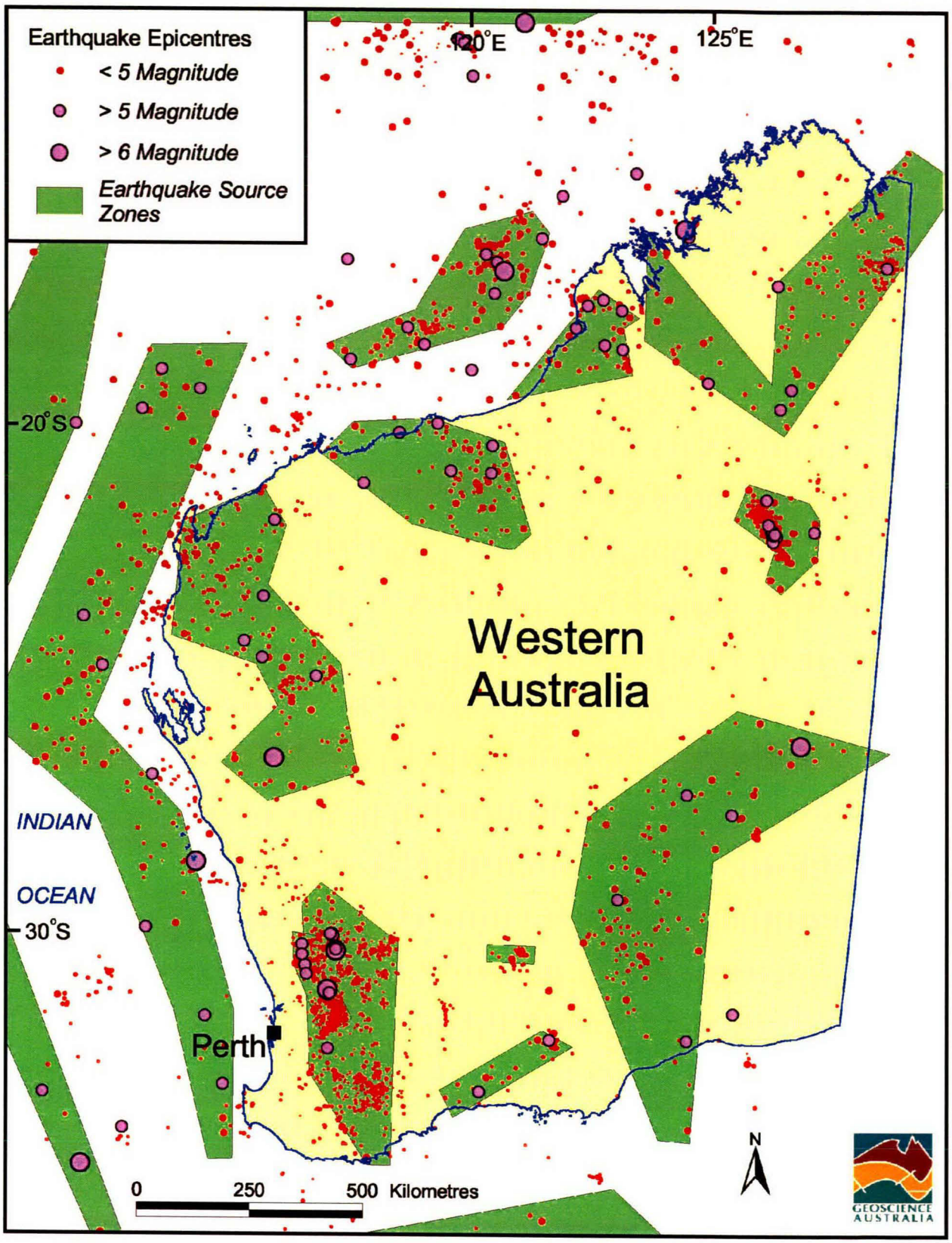

Figure C1: Earthquake epicentres and source zones for WA (from Gaull *et al.*, 1990)

The coordinates of the source zones were chosen by Gaul *et al.* according to the following criteria:

i) for zone 1, the western and southern boundaries to match the corresponding boundaries of the high grade metamorphic belts within the region;
ii) the shape of zones 2 was based primarily on the areal distribution of epicentres;
iii) offshore zones 3 and 4 are associated with the continental margin and 5000 m isobath respectively;
iv) zone 5 is correlated to a geological feature - the Fraser Fault; and
v) zone 6 is related to mine activity near Kalgoorlie.

A more detailed picture of the seismicity near Perth is shown on Fig. C2. Regions outside the source zones have sparse seismic activity.

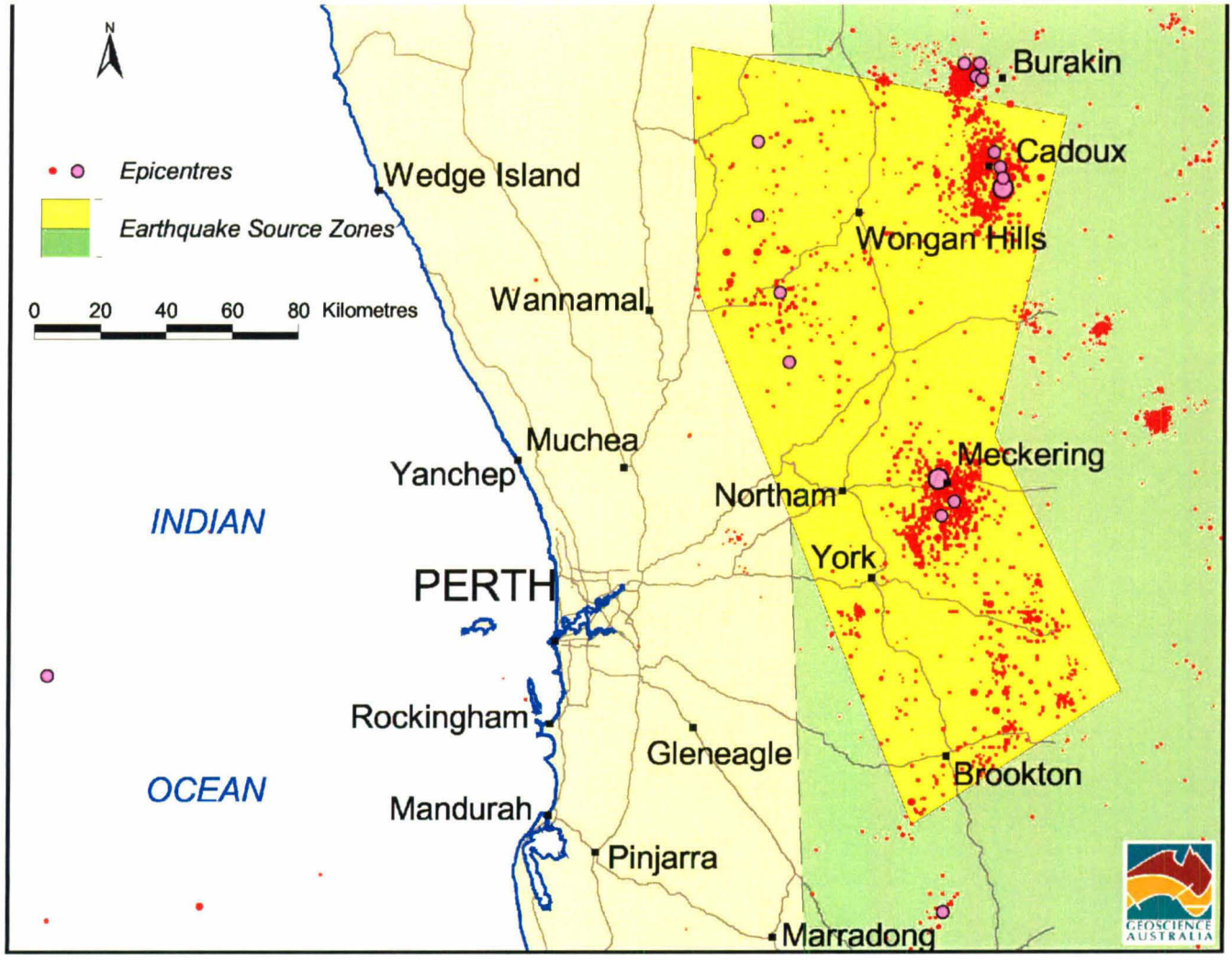

Figure C2: Detailed seismicity and zones near Perth (from Gaull *et al.*, 1990)

To aid in the characterisation of seismicity in SW Western Australia, another analysis of seismicity rates across Australia (Williams, N. and Leonard, M., 2001, Classifying the seismic regions of Australia, AEES Conference, Canberra) is given for comparison here. The primary goals of that analysis were to help define zones (Fig. C3) in which data quality was good enough for further analysis, and to determine the broad characteristics for large regions of Australia, which could be later subdivided and characterised in more details.

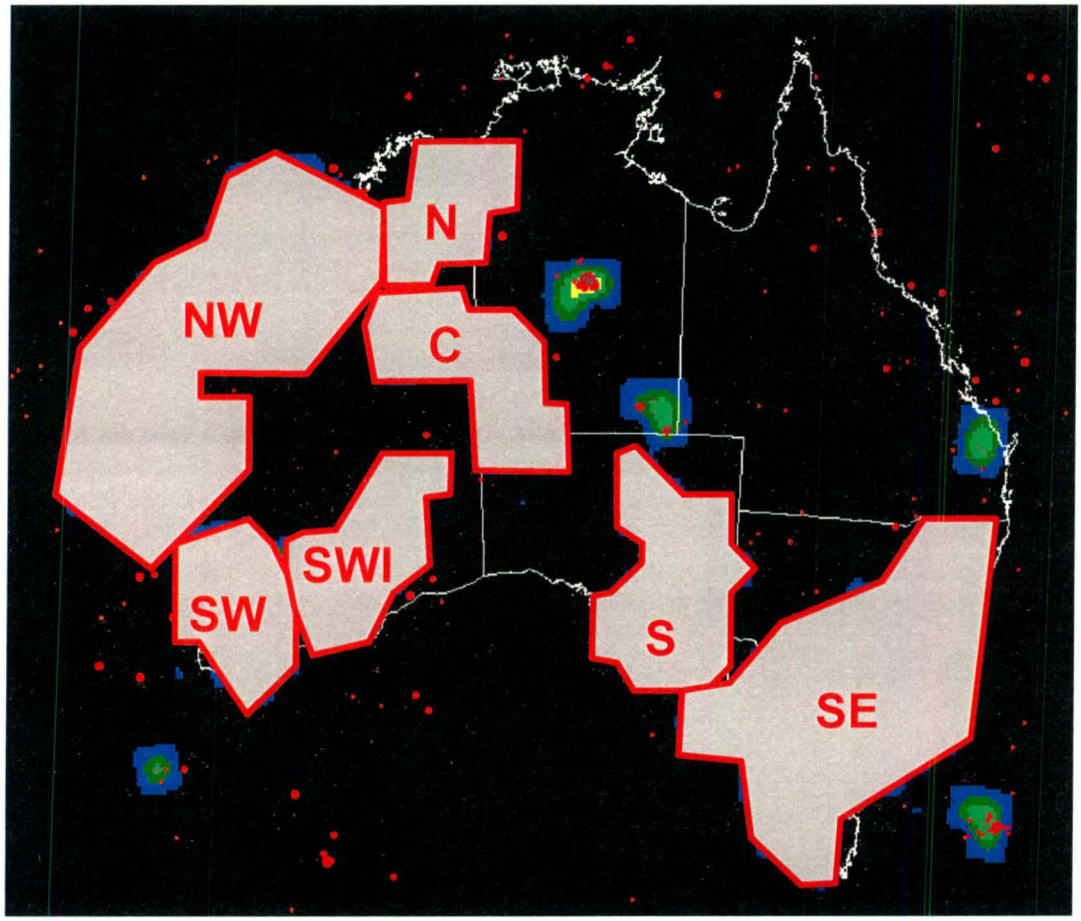

Figure C3: Map showing the partial definitions of seven zones for which boundaries are based purely on the limits of valid data. SW = southwest seismic zone; SWI = inland southwest zone; NW = northwest zone; N = northern zone; C = central zone; S = Adelaide Geosyncline; SE = southeast seismic zone.

APPENDIX D: CAUSES OF INTRA-PLATE SEISMICITY

Mike Dentith – edited by Dan Clark

I – Zone of weakness/resurgent tectonics;

II – Lateral density contrasts;

III – Contrasts in elastic properties;

IV – Increased heatflow.

The SWSZ occurs far from any plate boundary within an Archaean craton located in a stable continental interior. Therefore, this is an area of intra-plate seismicity by all accepted definitions; see for example Johnston (1989) and Talwani and Rajendran (1991).

Seismicity occurs where stress exceeds the mechanical strength of the crust. However, normally the stress levels in intra-plate areas of the continental lithosphere are not high enough to cause failure. This has led to the general acceptance that models for intra-plate seismicity must include a reason for the crust to be abnormally weak, and/or the stress to be locally amplified (Talwani, 1989). The stress amplification may occur through some mechanism that concentrates the effects of the ambient stress field, or may be due to the addition of some local source of stress acting in concert with the ambient field.

An important factor in assessing the models is that some mechanisms are necessarily of limited areal extent. Thus, some mechanisms might be applicable to an entire seismogenic region extending over distances of hundreds of kilometres, whilst other effects may only operate in areas measured in kilometres. Also, it is possible that more than one mechanism, or combination of mechanisms will be operating in a given area.

In considering the SWSZ some models for intra-plate seismicity can be immediately discounted. For example, those associated with isostatic uplift following the retreat of ice sheets, since the last glaciation in the region was during the Permian. Also unlikely to be important are stresses associated with the formation of passive continental margins. Although both the west and south coasts of Western Australia are margins of this type, the seismicity parallels neither.

Various models for intra-plate seismicity were reviewed in the context of the SWSZ, many of which have been developed to explain the seismicity in the eastern USA. The review of causes of intra-plate seismicity shows that numerous mechanisms have been proposed and although the evidence suggests that some can be dismissed with respect to the SWSZ, a number of possibilities remain.

1. ZONES OF WEAKNESS

In many explanations of intra-plate seismicity weak areas of the crust are envisaged to be pre-existing fault structures which if favourably oriented can be more easily reactivated than a new structure created (Sbar and Sykes, 1973; Sykes, 1978). In addition to favourable

orientation, selective reactivation may be related to variations in pore pressure, fault friction and localised deformation in the lower crust (Zoback, 1992b). The reactivation of faults (Fig. D1) is often referred to as 'resurgent tectonics', or the 'zone of weakness model', and the structures involved range from terrane boundaries through to comparatively minor faults.

Johnston and Kanter (1990) have shown that failed intracratonic rifts are the sites of a disproportionate amount of intra-plate seismicity, presumably because of the presence of geological characteristics that are particularly favourable for reactivation. In addition to faults, stratigraphic contacts, especially if there is a rheological contrast between different units, are also potential weak zones. A third possibility is that the rocks comprising the crust may be weakened by changes in, for example, pore pressure.

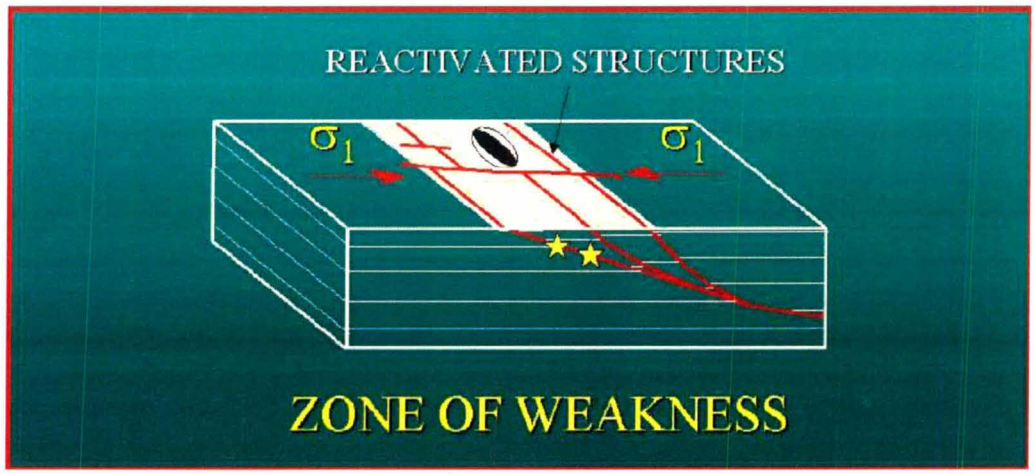

Figure D1: Schematic diagram of a zone of weakness

In considering zone of weakness, it is important to consider the scale of the structures involved. This is because weak zones such as existing faults and juxtaposition of different rock types are so common in the continental crust that whatever mechanism concentrates the stresses, failure is almost certain to occur on one of these. However, for a zone of weakness to be the dominant reason for the seismicity, it must affect the entire crust (Liu and Zoback, 1997), and hence this scenario is restricted to large-scale features such as terrane boundaries.

2. STRESS AMPLIFICATION DUE TO LOADING/BOUYANCY FORCES

Lateral Changes in Density

It is well established that bouyancy forces associated with topography and subsurface density changes can generate significant stresses, see for example, Artyushkov (1973), and Zoback (1992a). Such lateral changes in density, giving rises to loads that must be borne by the lithosphere, have been suggested as a mechanism for intra-plate seismicity. Figure D2 is an example of a mechanism where additional stresses are generated in addition to the ambient stress field.

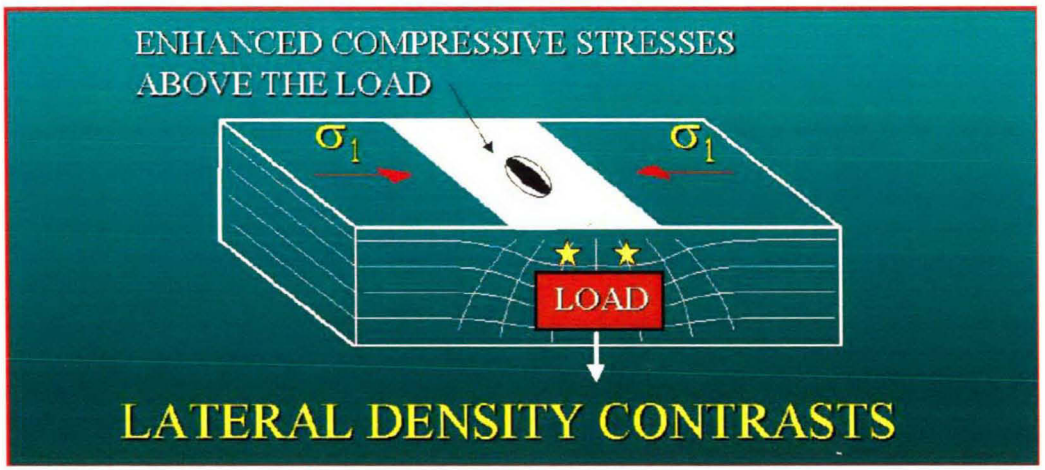

Figure D2: Schematic diagram of lateral density contrasts

Intra-plate seismicity in the Precambrian of southern India has been ascribed in part to stresses induced by topography and density heterogeneities (Mandal, 1999). Using the method of Kuang *et al.* (1989), Mandal (1999) calculates stresses caused by surface and Moho topography in southern India, although no account was taken of intra-crustal density variations, with all density contrasts assumed to concentrated at the base of the crust. The local seismicity was attributed to failure along existing fault lines under the combined stress effects of plate boundary forces and forces associated with local topographic and density variations.

The available seismic refraction data suggest that Moho relief is comparable to that in southern India to about 5 km (Dentith *et al.*, 2000). However, surface topographic variation is significantly smaller. Although the landscape in Western Australia is probably better defined than in India, quantitative study of the stresses caused by topography etc. is not currently possible since the geometry of the mid and base crust density contrasts is known only along a single profile. As noted previously, there is a correlation between seismicity and some aspects of the local topography, for example the area to the east of the region, the Darling Plateau. However, overall topography in the region is subdued and associated crustal loading unlikely to be a significant factor.

As noted above, a disproportionate amount of intra-plate seismicity is associated with palaeo-rifts. This may be due to the presence of "rift pillows"; areas of anomalously high seismic velocity and density, interpreted as zones of pervasive intrusion associated with crustal extension. The load associated with the dense material creates compressional stresses in the overlying crust, with the maximum stresses oriented perpendicular to the trend of the rift. The observed stress is due to a combination of the regional stress and that due to the load. The amount of both stress amplification and rotation depends on the load represented by the pillow, the physical properties of the surrounding lithosphere and the time since the load was applied. The maximum stresses occur above the thickest part of the pillow.

The high velocity zone (HVZ) beneath in the SWSZ could potentially cause similar effects to rift pillows and hence be responsible for some, or all, of the observed seismicity (Dentith *et al.*, 2000). It might also account for some of the second-order variations in stress direction. However, it is not suggested here that the HVZ is necessarily a rift pillow.

The important fact from the perspective of the SWSZ is that the zone represents a load and hence could be amplifying compressive stresses in the overlying crust. Whether the stress

rotation and amplification is significant awaits determination of the size and geometry of the HVZ and then modelling in the context of the local lithosphere. However, at this stage, a persuasive argument against it being a significant influence is the lack of subsidence in the overlying area. Also, for the reasons outlined above, it is probably of Precambrian age. Maintaining loading stresses within the crust for the required amount of time presents significant difficulties.

3. LATERAL CHANGES IN ELASTIC PROPERTIES

Another model for intra-plate seismicity involves the concentration of regional stress by lateral changes in elastic properties (see Campbell, 1978 and references therein). Variations in the elastic properties of the rocks passively modify the regional stress field, creating local concentrations of stress (Fig. D3). The mechanism is usually inferred from correlations between epicentres and potential field anomalies, interpreted as coinciding with intrusions. An example from the New Madrid Seismic Zone (NMSZ) is presented by Ravat *et al.* (1987) and an example from Ohio by Hinze *et al.* (1988). An alternative explanation for a localised weak zone in the crust is that its thermal and/or hydraulic properties are perturbed, for example by intrusion or increased fluid content (Gettings, 1988; Long and Zelt, 1991).

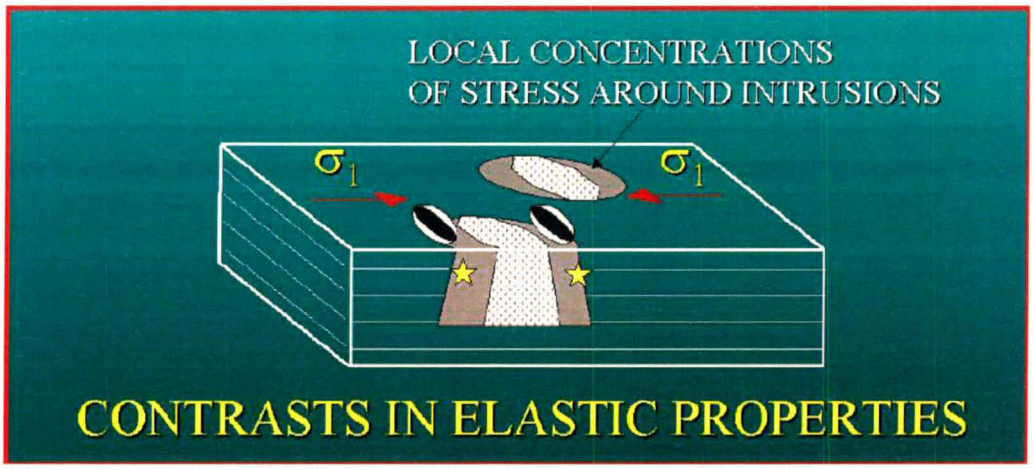

Figure D3: Schematic diagram of localised concentrations of stress

In the context of the SWSZ, the country rocks are basically gneisses. Intrusions of granitic and mafic/ultramafic rocks are known to occur in the area. There is overlap in the elastic properties of granites and gneisses and, in the absence of local measurements, it is unknown whether the intrusions are stronger or weaker than their surrounds. Mafic and ultramafic rocks are stronger than both gneisses and granites, however, serpentinisation makes mafic and ultramafic rocks comparatively weak.

The presence of sub-circular gravity lows in the SWSZ suggests granitic intrusions in the upper crust, and it has already been noted that seismicity tends to occur on the eastern and western margins of these anomalies. The HVZ in the lower crust is probably of mafic/ultramafic composition, hence is also a region whose elastic properties are likely to differ from its surrounds.

It may be significant that the cluster of epicentres at Meckering also occurs adjacent to a negative gravity anomaly, in a position consistent with the stress amplification due to the presence of a rigid body. This anomaly is of much larger diameter than that near Cadoux, and hence results in less stress amplification. However, the gravity data suggest there is a small

lobe on the western margin of the main anomaly, adjacent to the Meckering epicentre. A local stress concentration may be what triggered failure at this particular location, with or without a contribution from stress amplification due to intersecting faults.

4. THERMAL WEAKENING OF THE LOWER CRUST

An alternative form of the zone of weakness model, which also involves concentration of ambient stresses, is that described by Liu and Zoback (1997). These authors, using the NMSZ as an example, argue for a weak zone in the lower crust and upper mantle rather than the upper crust. Their model is based on evidence for higher subsurface temperatures in the NMSZ than surrounding areas, which causes the lower crust and upper mantle to be anomalously weak. Consequently, stresses become concentrated in the brittle upper crust, encouraging failure (Fig. D4).

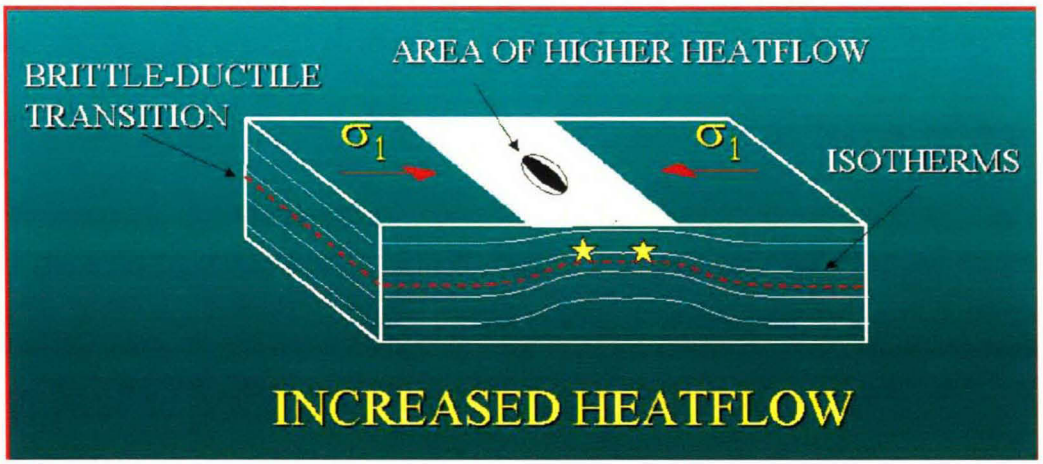

Figure D4: Schematic diagram of a higher heatflow condition

The applicability of the model of Liu and Zoback (1997) to the SWSZ can be tested based on available data. There is a reasonable amount of heatflow data from the Yilgarn Craton, including an approximately east-west trending traverse that crosses the SWSZ. These data show the heatflow in the Yilgarn Craton varying between about 30 and 55 mW/m^2. There is little correlation between seismicity and higher values of heatflow. For example, there are high values immediately to the east of the SWSZ, but a third reading that is within the zone itself is comparatively low. Moreover, other areas within the Craton with higher heatflow values are not associated with high levels of seismicity.

The seismic refraction study of the SWSZ and surrounding area described by Dentith *et al.* (2000) does not constrain the P-wave velocity of the mantle very well. However, it is possible to model the observed travel times with a comparatively high velocity at the Moho of about 8.2 km/s and without resorting to lateral changes in velocity. Finally, there is no evidence of a correlation between enhanced heatflow and subsidence, and most importantly, no topographic correlation with heatflow and no geological evidence for sediments that might have accumulated in low lying areas caused by thermal subsidence. Thus, the weight of evidence strongly suggests Lui and Zoback's (1997) model is not applicable to the SWSZ.

REFERENCES

Artyushkov, E.V., 1973. Stresses in the lithosphere caused by crustal thickness inhomogeneities. Journal of Geophysical Research, 78, 7675-7708.

Campbell, D.L., 1978. Investigation of the stress-concentration mechanism for intraplate earthquakes. Geophysical Research Letters, 5, 477-479.

Dentith, M.C., Dent, V.F., and Drummond, B.J., 2000. Deep crustal structure in the south western Yilgarn Craton, Western Australia. Tectonophysics, 325, 227-255.

Gettings, M.E., 1988. Variation of depth to the brittle-ductile transition due to cooling of a midcrustal intrusion. Geophysical Research Letters, 15, 213-216.

Hinze, W.J., Braile, L.W., Keller, G.R., and Lidiak, E.G., 1988. Model of mid-continent tectonism: An update. Reviews of Geophysics, 26, 699-717.

Johnston, A.C., 1989. The seismicity of "stable" continental interiors. In: S. Gregersen and P.W. Basham (Eds), Earthquakes at North Atlantic Passive Margins: Neotectonics and Glacial Rebound. Kluwer, 299-327.

Johnston, A.C., and Kanter, L.R., 1990. Earthquakes in stable continental crust. Scientific American, 262, 68-75.

Kuang, J., Long, J.T., and Mareschal, J.T., 1989. Intraplate seismicity and stress in the southeastern United States. Tectonophysics, 170, 29-42.

Liu, L., and Zoback, M.D., 1997. Lithospheric strength and intraplate seismicity in the New Madrid seismic zone. Tectonics, 16, 585-595.

Long, T.L., and Zelt, K., 1991. A local weaking of the brittle-ductile transition can explain some intraplate seismic zones. Tectonophysics, 186, 175-192.

Mandal, P., 1999. Intraplate stress distribution induced by topography and crustal density heterogeneities beneath the south Indian shield, India. Tectonophysics, 302, 159-172.

Ravat, D.N., Braile, L.W., and Hinze, W.J., 1987. Earthquakes and plutons in the midcontinent – evidence from the Bloomfield pluton, New Madrid rift complex. Seismological Research Letters, 58, 41-52.

Sbar, M.L., and Sykes, L.R., 1973. Contemporary compressive stress and seismicity in eastern North America: An example of intra-plate tectonics. Geological Society of America Bulletin, 84, 1861-1882.

Sykes, L.R., 1978. Intraplate seismicity, reactivation of preexisting zones of weakness, alkaline magmatism, and other tectonism postdating continental fragmentation. Reviews of Geophysics and Space Physics, 16, 621-688.

Talwani, P., 1989. Characteristic features of intraplate earthquakes and the models proposed to explain them. In, Earthquakes at North–Atlantic passive margins: Neotectonics and

Postglacial rebound, S. Gregerson and P.W. Basham (Eds), Kluwer Academic publishers, 563-579.

Talwani, P., and Rajendran, K., 1991. Some seismological and geometric features of intraplate earthquakes. Tectonophysics, 186, 19-41.

Zoback, M.L., 1992a. First- and second-order patterns of stress in the lithosphere: The world stress map project. Journal of Geophysical Research, 97, 11703-11728.

Zoback, M.L., 1992b. Stress field constraints on intraplate seismicity in eastern North America. Journal of Geophysical Research, 97, 11761-11782.